State convergence theory applied to a nonlinear and delayed telerobotic system

Julio C. Tafur · Cecilia García · Rafael Aracil · Roque Saltaren

Abstract State convergence is a control strategy that was proposed in the early 2000s to ensure stability and transparency in a teleoperation system under specific control gains values. This control strategy has been implemented for a linear system with or without time delay. This paper represents the first attempt at demonstrating, theoretically and experimentally, that this control strategy can also be applied to a nonlinear teleoperation system with n degrees of freedom and delay in the communication channel. It is assumed that the human operator applies a constant force on the local manipulator during the teleoperation. In addition, the interaction between the remote manipulator and the environment is considered passive. Communication between the local and remote sites is made by means of a communication channel with variable time delay. In this article the theory of Lyapunov–Krasovskii was used to demonstrate that the local–remote teleoperation system is asymptotically stable.

Keywords Lyapunov–Krasovskii · Nonlinear control · Stability · Telerobotic · Time delay

1 Introduction

Teleoperation has been an active research topic since Goertz and Thompson's demonstration of their first *master–slave* remote control in 1954 [1]. These kinds of systems are used in many different applications related to robotics, such as the handling of toxic or harmful materials, operations in remote environments, surgery, submarines, and activities in space [2].

A teleoperation system consists of a master device, a remote device, and a communication channel that controls the transfer of force and velocity information. The human operator controls the remote robot by manipulating

J. C. Tafur
Departamento de Ingeniería, Pontificia Universidad Católica del Perú, Lima 32, Lima, Peru
e-mail: jtafur@pucp.edu.pe

C. García (✉) · R. Aracil · R. Saltaren
Centre for Automation and Robotics, Universidad Politécnica de Madrid, 28006 Madrid, Spain
e-mail: cecilia.garcia@upm.es

C. García
Escuela Técnica Superior de Ingeniería y Diseño Industrial, Universidad Politécnica de Madrid, Madrid, Spain

the local device. Typically, bidirectional communication between master and slave is performed over the Internet [Transmission Control Protocol/Internet Protocol (TCP/IP)]; however, some applications may require a dedicated communication link.

Stability is one of the most important properties of any robotic system. In teleoperation, stability is associated with the property of telepresence, which enables the human to be virtually present at the remote location [3]. There is an inherent tradeoff between these two properties: telepresence improves with increased feedback from the remote manipulator; therefore, if the system exhibits unstable or nearly unstable behavior, telepresence cannot be ensured.

On the other hand, the communication channel plays an important role in stability and telepresence properties. The use of the Internet and other packet-switched networks, such as Internet2, imposes time-varying delays on control systems. New control schemes must be proposed to deal with the instabilities caused by these time-varying delays to ensure good performance in teleoperation tasks.

In the past, the instability introduced by time delays required that the system be controlled in an *open-loop mode*, reducing the technique of the operator to that of wait and see [4–6]. When designing a control system for teleoperation, this latency introduces a conflict between stability and performance.

Furthermore, because the Internet has become the most common communication channel for teleoperation, time delays have become variable delays. A significant amount of research effort has been devoted to developing novel control methods to deal with the time-varying delays inherent in the TCP or User Datagram Protocol (UDP).

For instance, Li and Su [7] investigated an adaptive neural network control for single-master–multiple-slave teleoperation while considering time delays and input dead-zone uncertainties for multiple mobile manipulators carrying a common object in a cooperative manner. The developed control approach ensures that the defined tracking errors converge to zero, whereas the coordination internal force errors remain bounded and can be made arbitrarily small. Throughout this paper, stability analysis is performed via explicit Lyapunov techniques under specific linear matrix inequality (LMI) conditions.

In [8] an adaptive fuzzy control scheme for the hybrid motion/force of a trilateral teleoperation system is proposed. The system consists of a dual-master–single-slave configuration under stochastic time-varying delays in communication channels. It is proven that the trilateral teleoperation system is stochastically stable in mean square under specific LMI conditions, and all the signals of the resulting closed-loop system are uniformly bounded.

Li et al. [9] consider the position/force control of bilateral teleoperation systems subject to time-varying delays and dynamical uncertainties. The stability of the closed-loop system and the boundedness of synchronization tracking errors are proved using LMI based on Lyapunov stability synthesis. The position/force tracking error up to an ultimately bounded error is achieved. Their work is expanded [10] by examining an adaptive control scheme for master–slave teleoperation systems with dynamical uncertainties and unsymmetrical time-varying delays in communication channels. The stability of two subsystems is proved with LMIs based on Lyapunov stability synthesis.

Hashemzadeh et al. [11] proposed a new adaptive controller design scheme for nonlinear telerobotic systems with time-varying delays where the delays and their variation rates are unknown. It is shown that position and velocity errors between the local and remote manipulators converge to zero asymptotically, thereby ensuring teleoperation transparency.

The problem of position tracking in the presence of time-varying delay was analyzed in [12]. A Lyapunov function is proposed to analyze the stable behavior of teleoperation systems, which is slightly modified under different control schemes such as P-like, PD-like, and scattering transformation.

However, this analysis considers the classic assumption of the passivity of the operator, which leads to a more restrictive model of the human operator.

1.1 Evolution of control by state convergence

To develop a state convergence method for a teleoperation system, the whole system must be taken into account: the local operator, the local manipulator handled by the local operator, the remote manipulator, and the environment.

The state convergence control scheme for teleoperation systems considers all possible interactions that could occur in the operator-local-remote-environment set (Fig. 2).

The state convergence method provides an alternative for designing bilateral controllers. This method was proposed by researchers from Universidad Politécnica de Madrid and Miguel Hernández University in the early 2000s.

The importance and novelty of the design method presented in [5] lies in the possibility of obtaining a control scheme so that the dynamics of the slave, as well as the dynamics of the state convergence of the master and the slave, result in the desired behavior regardless of any time delay in the communication channel, the constant reflection efforts, and the dynamic characteristics of master, slave, and the environment.

The method has been validated experimentally in a linear teleoperated system [5] with 2 degrees of freedom (DOFs), where the master robot structure differs from that of the slave [13]. Studies have also been carried out using adaptive control strategies based on this control scheme [14] and on designs contemplating delays in transmission [4].

In the control scheme proposed by [5] for first-order linear systems and [15] for n-order linear systems, position drift arises from two sources: the use of a linear system model, which requires that the dynamic model of the teleoperator be precisely known in order to determine the controller gains, and the use of a first-order Taylor expansion to approximate the time delays.

In [14] a new version of the control scheme based on [5] is presented for the design of a bilateral controller based on an adaptive concept. The scheme includes some additional scalar gains and matrices that feed slave–environment interaction back to the master. The analysis considers only first-order linear systems; communication time delays are not considered. The authors conclude that, using this scheme, ideal transparency cannot be obtained because it derives from noncausal systems. They present the experimental results to validate the method, but these have only been applied to a 1-DOF linear system.

In previous articles [16,17], the authors presented state convergence control methods for a nonlinear, bilateral teleoperation system with n DOFs. In the first article, the authors analyzed the stability of a closed-loop system, whereas in the latter, simulation results were presented to confirm the theoretical results. Moreover, [17] includes the outline of the mechanical setup employed for real-time experiments.

This proposal relies on demonstrating that the structure of a state convergence algorithm [15] can also be applied to nth-order nonlinear teleoperation systems and attempts to improve the position signal as presented in [15], which demonstrated drift problems.

The main contributions of this article are as follows:

a. To demonstrate that a state convergence control scheme can, theoretically, be applied to *n-order* nonlinear telerobotic systems under variable time delays.
b. To demonstrate the asymptotical stability of a nonlinear system for both local and remote manipulation with a variable time delay.
c. To show that the control scheme can be implemented in real time.
d. To validate the experimental control gains against the theoretically determined gains for the proposed control scheme.
e. To show experimentally that the proposed control scheme ensures the asymptotical stability of the system for both local and remote manipulation with a variable time delay.

This article is organized in six sections. The mathematical model of the teleoperator system is described in Sect. 2. The control scheme and stability analysis are presented in Sect. 3. Computer simulations of the proposed control scheme are presented in Sect. 4. Experimental results are given in Sect. 5, and conclusions are drawn in Sect. 6.

2 Nonlinear model of n-DOF teleoperation system

Let us consider a robot manipulator on n DOFs composed of rigid links interconnected by frictionless joints. If $\mathbf{q}, \dot{\mathbf{q}} \in \mathbf{R}^n$ are position and velocity vectors, then the kinetic energy $\mathbf{K}(\mathbf{q}, \dot{\mathbf{q}})$ associated to this articulated mechanism

can be expressed by

$$\mathbf{K}(\mathbf{q}, \dot{\mathbf{q}}) = \frac{1}{2}\dot{\mathbf{q}}^{\mathrm{T}}\mathbf{M}(\mathbf{q})\dot{\mathbf{q}},$$

where $\mathbf{M}(\mathbf{q}) \in \mathbf{R}^{n\times n}$ is the symmetric and positive-definite inertia matrix. On the other hand, the potential energy $\mathbf{U}(\mathbf{q})$ depends only on the position vector.

The Lagrange equations of motion may be written as

$$\frac{\mathrm{d}}{\mathrm{d}t}\left(\frac{\partial}{\partial\dot{\mathbf{q}}}\left(\frac{1}{2}\dot{\mathbf{q}}^{T}\mathbf{M}(\mathbf{q})\dot{\mathbf{q}}\right)\right) - \frac{\partial}{\partial\mathbf{q}}\left(\frac{1}{2}\dot{\mathbf{q}}^{T}\mathbf{M}(\mathbf{q})\dot{\mathbf{q}}\right) + \frac{\partial\mathbf{U}(\mathbf{q})}{\partial\mathbf{q}} = \boldsymbol{\tau},$$

where $\boldsymbol{\tau}$ is the vector of external forces.

Then, we have the following:

$$\mathbf{M}(\mathbf{q})\ddot{\mathbf{q}} + \dot{\mathbf{M}}(\mathbf{q})\dot{\mathbf{q}} - \frac{1}{2}\frac{\partial}{\partial\mathbf{q}}\left(\dot{\mathbf{q}}^{\mathrm{T}}\mathbf{M}(\mathbf{q})\dot{\mathbf{q}}\right) + \frac{\partial\mathbf{U}(\mathbf{q})}{\partial\mathbf{q}} = \boldsymbol{\tau}$$

or

$$\mathbf{M}(\mathbf{q})\ddot{\mathbf{q}} + \mathbf{C}(\mathbf{q}, \dot{\mathbf{q}})\dot{\mathbf{q}} + \mathbf{g}(\mathbf{q}) = \boldsymbol{\tau},$$

where

$$\mathbf{C}(\mathbf{q}, \dot{\mathbf{q}})\dot{\mathbf{q}} = \dot{\mathbf{M}}(\mathbf{q})\dot{\mathbf{q}} - \frac{1}{2}\frac{\partial}{\partial\mathbf{q}}\left(\dot{\mathbf{q}}^{\mathrm{T}}\mathbf{M}(\mathbf{q})\dot{\mathbf{q}}\right),$$

$$\mathbf{g}(\mathbf{q}) = \frac{\partial\mathbf{U}(\mathbf{q})}{\partial\mathbf{q}}.$$

The dynamics of a robot manipulator involves nonlinear terms such as inertial, Coriolis/centripetal, friction, or gravitational forces that depend on trigonometric functions in a complex way.

Consider the generic configuration of an articulated arm of n links as shown in Fig. 1. The local and remote manipulators for a teleoperation system are n-DOF manipulators described by Euler–Lagrange equations of the form

$$\mathbf{M}_{\mathrm{l}}(\mathbf{q}_{\mathrm{l}})\ddot{\mathbf{q}}_{\mathrm{l}} + \mathbf{C}_{\mathrm{l}}(\mathbf{q}_{\mathrm{l}}, \dot{\mathbf{q}}_{\mathrm{l}})\dot{\mathbf{q}}_{\mathrm{l}} + \mathbf{g}_{\mathrm{l}}(\mathbf{q}_{\mathrm{l}}) = \boldsymbol{\tau}_{\mathrm{lc}} + \mathbf{F}_{\mathrm{h}}, \qquad \mathbf{M}_{\mathrm{r}}(\mathbf{q}_{\mathrm{r}})\ddot{\mathbf{q}}_{\mathrm{r}} + \mathbf{C}_{\mathrm{r}}(\mathbf{q}_{\mathrm{r}}, \dot{\mathbf{q}}_{\mathrm{r}})\dot{\mathbf{q}}_{\mathrm{r}} + \mathbf{g}_{\mathrm{r}}(\mathbf{q}_{\mathrm{r}}) = \boldsymbol{\tau}_{\mathrm{rc}} - \mathbf{F}_{\mathrm{e}}, \tag{1}$$

where $\ddot{\mathbf{q}}_i, \dot{\mathbf{q}}_i, \mathbf{q}_i \in \mathbf{R}^n$ represent respectively the acceleration, velocity, and position of the joint i = {l, r}, where the l and r subindices represent the local and remote manipulators, respectively. $\mathbf{M}_i(\mathbf{q}_i) \in \mathbf{R}^{n\times n}$ represents a generalized inertia matrix, $\mathbf{C}_i(\mathbf{q}_i, \dot{\mathbf{q}}_i) \in \mathbf{R}^{n\times n}$ is the Coriolis and centrifugal forces matrix, $\mathbf{g}_i(\mathbf{q}_i) \in \mathbf{R}^n$ denotes the gravitational vector, $\boldsymbol{\tau}_{\mathrm{ic}} \in \mathbf{R}^n$ is the control torque signal, $\mathbf{F}_{\mathrm{h}} \in \mathbf{R}^n$ represents the human operator interaction force and, finally, $\mathbf{F}_{\mathrm{e}} \in \mathbf{R}^n$ is the environment interaction force.

Assumption 1 The human operator applies a constant force in the closed-loop system and can be expressed as

$$\mathbf{F}_{\mathrm{h}} = \mathbf{F}_{\mathrm{op}}. \tag{2}$$

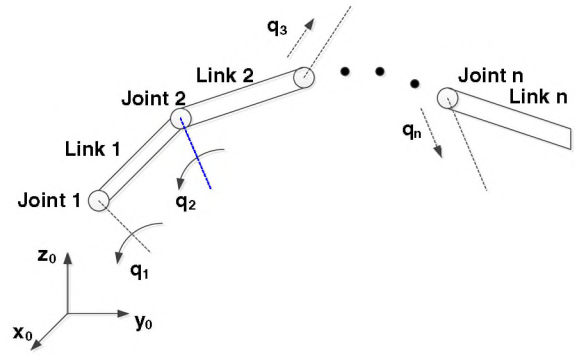

Fig. 1 Schematic diagram of n-DOF robot manipulator

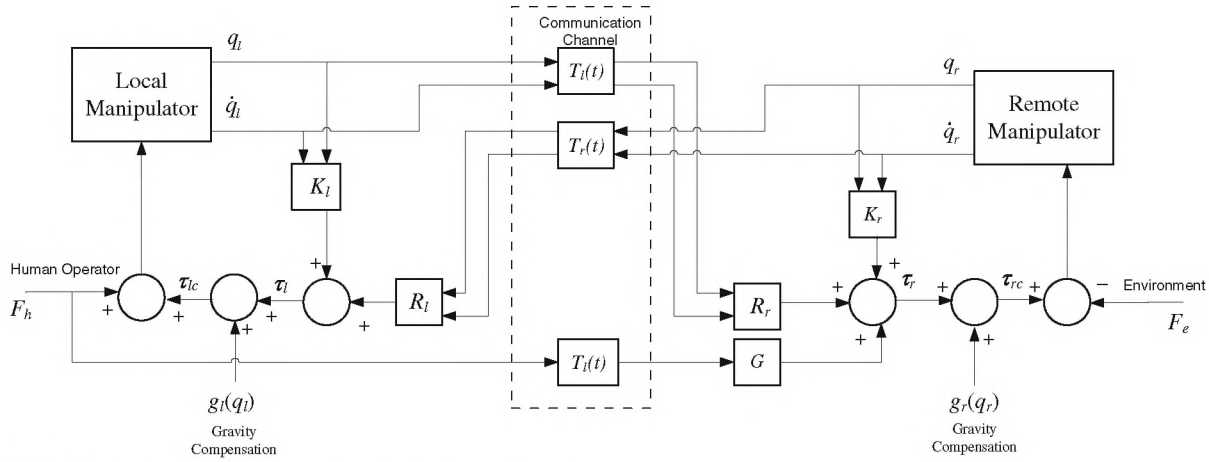

Fig. 2 Block diagram of nonlinear control of teleoperation system

Assumption 2 The interaction between the environment and the remote robot is passive:

$$\mathbf{F}_{\mathrm{e}} = \mathbf{K}_{\mathrm{e}}\mathbf{q}_{\mathrm{r}} + \mathbf{B}_{\mathrm{e}}\dot{\mathbf{q}}_{\mathrm{r}}, \tag{3}$$

where $\mathbf{K}_{\mathrm{e}}$ and $\mathbf{B}_{\mathrm{e}}$ are positive-definite matrices $\in \mathbf{R}^{n\times n}$.

From Fig. 2 it can be seen that the proposed control law compensates for gravitational forces; therefore, the control torques $\boldsymbol{\tau}_{\mathrm{ic}}$ are given by

$$\boldsymbol{\tau}_{\mathrm{lc}} = \boldsymbol{\tau}_{\mathrm{l}} + \mathbf{g}_{\mathrm{l}}(\mathbf{q}_{\mathrm{l}}), \quad \boldsymbol{\tau}_{\mathrm{rc}} = \boldsymbol{\tau}_{\mathrm{r}} + \mathbf{g}_{\mathrm{r}}(\mathbf{q}_{\mathrm{r}}). \tag{4}$$

By replacing (4) in (1), the closed-loop system can be expressed as

$$\mathbf{M}_{\mathrm{l}}(\mathbf{q}_{\mathrm{l}})\ddot{\mathbf{q}}_{\mathrm{l}} + \mathbf{C}_{\mathrm{l}}(\mathbf{q}_{\mathrm{l}}, \dot{\mathbf{q}}_{\mathrm{l}})\dot{\mathbf{q}}_{\mathrm{l}} = \boldsymbol{\tau}_{\mathrm{l}} + \mathbf{F}_{\mathrm{op}}, \qquad \mathbf{M}_{\mathrm{r}}(\mathbf{q}_{\mathrm{r}})\ddot{\mathbf{q}}_{\mathrm{r}} + \mathbf{C}_{\mathrm{r}}(\mathbf{q}_{\mathrm{r}}, \dot{\mathbf{q}}_{\mathrm{r}})\dot{\mathbf{q}}_{\mathrm{r}} = \boldsymbol{\tau}_{\mathrm{r}} - \mathbf{F}_{\mathrm{e}}. \tag{5}$$

3 State convergence algorithm with variable time delay

Let us consider the new proposal for the state convergence method with time-varying delay for nonlinear systems, as shown in Fig. 2. The local and remote manipulators (1) are connected via a communication channel with a variable time delay, $T_i(t)$, $i = \{\mathrm{l}, \mathrm{r}\}$, and the torque for the local and remote manipulators is given by

$$\begin{aligned}
\boldsymbol{\tau}_{\mathrm{l}} &= \mathbf{K}_{\mathrm{l}1}\mathbf{q}_{\mathrm{l}} + \mathbf{K}_{\mathrm{l}2}\dot{\mathbf{q}}_{\mathrm{l}} + \mathbf{R}_{\mathrm{l}1}\mathbf{q}_{\mathrm{r}}(t - T_{\mathrm{r}}(t)) + \mathbf{R}_{\mathrm{l}2}\dot{\mathbf{q}}_{\mathrm{r}}(t - T_{\mathrm{r}}(t)),\\
\boldsymbol{\tau}_{\mathrm{r}} &= \mathbf{K}_{\mathrm{r}1}\mathbf{q}_{\mathrm{r}} + \mathbf{K}_{\mathrm{r}2}\dot{\mathbf{q}}_{\mathrm{r}} + \mathbf{R}_{\mathrm{r}1}\mathbf{q}_{\mathrm{l}}(t - T_{\mathrm{l}}(t)) + \mathbf{R}_{\mathrm{r}2}\dot{\mathbf{q}}_{\mathrm{l}}(t - T_{\mathrm{l}}(t)) + G\mathbf{F}_{\mathrm{op}}(t - T_{\mathrm{l}}(t)).
\end{aligned} \tag{6}$$

$\mathbf{K}_{\mathrm{l}} = [\,\mathbf{K}_{\mathrm{l}1}\ \mathbf{K}_{\mathrm{l}2}\,]$, $\mathbf{R}_{\mathrm{l}} = [\,\mathbf{R}_{\mathrm{l}1}\ \mathbf{R}_{\mathrm{l}2}\,]$, $\mathbf{K}_{\mathrm{r}} = [\,\mathbf{K}_{\mathrm{r}1}\ \mathbf{K}_{\mathrm{r}2}\,]$, $\mathbf{R}_{\mathrm{r}} = [\,\mathbf{R}_{\mathrm{r}1}\ \mathbf{R}_{\mathrm{r}2}\,]$, and $\mathbf{K}_{\mathrm{l}1}$, $\mathbf{K}_{\mathrm{l}2}$, $\mathbf{R}_{\mathrm{l}1}$, $\mathbf{R}_{\mathrm{l}2}$, $\mathbf{K}_{\mathrm{r}1}$, $\mathbf{K}_{\mathrm{r}2}$, $\mathbf{R}_{\mathrm{r}1}$, and $\mathbf{R}_{\mathrm{r}2}$ are order $n \times n$ gain matrices. G is a constant.

$\mathbf{K}_{\mathrm{l}}$ is the feedback matrix of the local manipulator state, $\mathbf{K}_{\mathrm{r}}$ is the feedback matrix of the remote manipulator state and models the interaction force between the remote manipulator and the environment, $\mathbf{R}_{\mathrm{l}}$ represents the reflection force from the remote manipulator to the local manipulator, $\mathbf{R}_{\mathrm{r}}$ models the interaction between local–remote manipulators, and G is a constant that reflects to the remote manipulator the force that the operator applies to the local manipulator.

Taking into account assumptions 1 and 2 and substituting (6) into (5) yield

$$\begin{aligned}
\mathbf{M}_{\mathrm{l}}(\mathbf{q}_{\mathrm{l}})\ddot{\mathbf{q}}_{\mathrm{l}} + \mathbf{C}_{\mathrm{l}}(\mathbf{q}_{\mathrm{l}}, \dot{\mathbf{q}}_{\mathrm{l}})\dot{\mathbf{q}}_{\mathrm{l}} &= \mathbf{K}_{\mathrm{l1}}\mathbf{q}_{\mathrm{l}} + \mathbf{K}_{\mathrm{l2}}\dot{\mathbf{q}}_{\mathrm{l}} + \mathbf{R}_{\mathrm{l1}}\mathbf{q}_{\mathrm{r}}(t - T_{\mathrm{r}}(t)) + \mathbf{R}_{\mathrm{l2}}\dot{\mathbf{q}}_{\mathrm{r}}(t - T_{\mathrm{r}}(t)) + \mathbf{F}_{\mathrm{op}}, \\
\mathbf{M}_{\mathrm{r}}(\mathbf{q}_{\mathrm{r}})\ddot{\mathbf{q}}_{\mathrm{r}} + \mathbf{C}_{\mathrm{r}}(\mathbf{q}_{\mathrm{r}}, \dot{\mathbf{q}}_{\mathrm{r}})\dot{\mathbf{q}}_{\mathrm{r}} &= \mathbf{K}_{\mathrm{r1}}\mathbf{q}_{\mathrm{r}} + \mathbf{K}_{\mathrm{r2}}\dot{\mathbf{q}}_{\mathrm{r}} + \mathbf{R}_{\mathrm{r1}}\mathbf{q}_{\mathrm{l}}(t - T_{\mathrm{l}}(t)) + \mathbf{R}_{\mathrm{r2}}\dot{\mathbf{q}}_{\mathrm{l}}(t - T_{\mathrm{l}}(t)) \\
&\quad + G\mathbf{F}_{\mathrm{op}}(t - T_{\mathrm{l}}(t)) - \mathbf{K}_{\mathrm{e}}\mathbf{q}_{\mathrm{r}} - \mathbf{B}_{\mathrm{e}}\dot{\mathbf{q}}_{\mathrm{r}}.
\end{aligned} \tag{7}$$

The position equilibrium points for both robots are defined by $\bar{\mathbf{q}}_{\mathrm{l}} \in \mathbf{R}^n$ and $\bar{\mathbf{q}}_{\mathrm{r}} \in \mathbf{R}^n$. In equilibrium, the system dynamics satisfy $\dot{\mathbf{q}}_{\mathrm{l}} = \dot{\mathbf{q}}_{\mathrm{r}} = \ddot{\mathbf{q}}_{\mathrm{l}} = \ddot{\mathbf{q}}_{\mathrm{r}} = \mathbf{0}$. Furthermore, in these equilibrium points it can be established that $\mathbf{q}_{\mathrm{l}} = \mathbf{q}_{\mathrm{l}}(t - T_{\mathrm{l}}(t)) = \bar{\mathbf{q}}_{\mathrm{l}}$, $\mathbf{q}_{\mathrm{r}} = \mathbf{q}_{\mathrm{r}}(t - T_{\mathrm{r}}(t)) = \bar{\mathbf{q}}_{\mathrm{r}}$, and $\mathbf{F}_{\mathrm{op}}$ is a constant. Substituting the last expressions into (7), the equilibrium points $\bar{\mathbf{q}}_{\mathrm{l}}$ and $\bar{\mathbf{q}}_{\mathrm{r}}$ satisfy

$$\mathbf{0} = \mathbf{K}_{\mathrm{l1}}\bar{\mathbf{q}}_{\mathrm{l}} + \mathbf{R}_{\mathrm{l1}}\bar{\mathbf{q}}_{\mathrm{r}} + \mathbf{F}_{\mathrm{op}}, \qquad \mathbf{0} = \mathbf{K}_{\mathrm{r1}}\bar{\mathbf{q}}_{\mathrm{r}} + \mathbf{R}_{\mathrm{r1}}\bar{\mathbf{q}}_{\mathrm{l}} + G\mathbf{F}_{\mathrm{op}}(t - T_{\mathrm{l}}(t)) - \mathbf{K}_{\mathrm{e}}\bar{\mathbf{q}}_{\mathrm{r}}. \tag{8}$$

The main goal of this work is to characterize and study the stability of a nonlinear teleoperator system. To simplify the mathematical demonstration, it is convenient to assign the reference origin of the system, that is, $[\mathbf{0}] \in \mathbf{R}^n$, as the equilibrium point of the system. Therefore, it is necessary to apply a coordinate transformation in the following way:

$$\tilde{\mathbf{q}}_{\mathrm{l}}(t) = \mathbf{q}_{\mathrm{l}}(t) - \bar{\mathbf{q}}_{\mathrm{l}} \rightarrow \mathbf{q}_{\mathrm{l}}(t) = \tilde{\mathbf{q}}_{\mathrm{l}} + \bar{\mathbf{q}}_{\mathrm{l}}, \tag{9}$$

$$\tilde{\mathbf{q}}_{\mathrm{r}}(t) = \mathbf{q}_{\mathrm{r}}(t) - \bar{\mathbf{q}}_{\mathrm{r}} \rightarrow \mathbf{q}_{\mathrm{r}}(t) = \tilde{\mathbf{q}}_{\mathrm{r}} + \bar{\mathbf{q}}_{\mathrm{r}}. \tag{10}$$

The new variables $\tilde{\mathbf{q}}_{\mathrm{l}}(t)$ and $\tilde{\mathbf{q}}_{\mathrm{r}}(t)$ represent a system with equilibrium at the origin. Since $\bar{\mathbf{q}}_{\mathrm{l}}$ and $\bar{\mathbf{q}}_{\mathrm{r}}$ are constant values, then from (8) and (9) we obtain

$$\begin{aligned}
&\dot{\mathbf{q}}_{\mathrm{l}}(t) = \dot{\tilde{\mathbf{q}}}_{\mathrm{l}}(t), \quad \dot{\mathbf{q}}_{\mathrm{r}}(t) = \dot{\tilde{\mathbf{q}}}_{\mathrm{r}}(t), \quad \ddot{\mathbf{q}}_{\mathrm{l}}(t) = \ddot{\tilde{\mathbf{q}}}_{\mathrm{l}}(t), \quad \ddot{\mathbf{q}}_{\mathrm{r}}(t) = \ddot{\tilde{\mathbf{q}}}_{\mathrm{r}}(t), \\
&\mathbf{q}_{\mathrm{l}}(t - T_{\mathrm{l}}(t)) = \tilde{\mathbf{q}}_{\mathrm{l}}(t - T_{\mathrm{l}}(t)) + \bar{\mathbf{q}}_{\mathrm{l}}, \qquad \mathbf{q}_{\mathrm{r}}(t - T_{\mathrm{r}}(t)) = \tilde{\mathbf{q}}_{\mathrm{r}}(t - T_{\mathrm{r}}(t)) + \bar{\mathbf{q}}_{\mathrm{r}}.
\end{aligned}$$

Substituting (9), (10) and the above equations into the closed-loop dynamics (7) we obtain

$$\begin{aligned}
\mathbf{M}_{\mathrm{l}}\ddot{\tilde{\mathbf{q}}}_{\mathrm{l}} + \mathbf{C}_{\mathrm{l}}\dot{\tilde{\mathbf{q}}}_{\mathrm{l}} &= \mathbf{K}_{\mathrm{l1}}(\tilde{\mathbf{q}}_{\mathrm{l}} + \bar{\mathbf{q}}_{\mathrm{l}}) + \mathbf{K}_{\mathrm{l2}}\dot{\tilde{\mathbf{q}}}_{\mathrm{l}} + \mathbf{R}_{\mathrm{l1}}(\tilde{\mathbf{q}}_{\mathrm{r}}(t - T_{\mathrm{r}}(t)) + \bar{\mathbf{q}}_{\mathrm{r}}) + \mathbf{R}_{\mathrm{l2}}\dot{\tilde{\mathbf{q}}}_{\mathrm{r}}(t - T_{\mathrm{r}}(t)) + \mathbf{F}_{\mathrm{op}}, \\
\mathbf{M}_{\mathrm{r}}\ddot{\tilde{\mathbf{q}}}_{\mathrm{r}} + \mathbf{C}_{\mathrm{r}}\dot{\tilde{\mathbf{q}}}_{\mathrm{r}} &= \mathbf{K}_{\mathrm{r1}}(\tilde{\mathbf{q}}_{\mathrm{r}} + \bar{\mathbf{q}}_{\mathrm{r}}) + \mathbf{K}_{\mathrm{r2}}\dot{\tilde{\mathbf{q}}}_{\mathrm{r}} + \mathbf{R}_{\mathrm{r1}}(\tilde{\mathbf{q}}_{\mathrm{l}}(t - T_{\mathrm{l}}(t)) + \bar{\mathbf{q}}_{\mathrm{l}}) + \mathbf{R}_{\mathrm{r2}}\dot{\tilde{\mathbf{q}}}_{\mathrm{l}}(t - T_{\mathrm{l}}(t)) \\
&\quad + G\mathbf{F}_{\mathrm{op}}(t - T_{\mathrm{l}}(t)) - \mathbf{K}_{\mathrm{e}}(\tilde{\mathbf{q}}_{\mathrm{r}} + \bar{\mathbf{q}}_{\mathrm{r}}) - \mathbf{B}_{\mathrm{e}}\dot{\tilde{\mathbf{q}}}_{\mathrm{r}}.
\end{aligned}$$

Grouping terms and using (8) yields

$$\begin{aligned}
\mathbf{M}_{\mathrm{l}}\ddot{\tilde{\mathbf{q}}}_{\mathrm{l}} + \mathbf{C}_{\mathrm{l}}\dot{\tilde{\mathbf{q}}}_{\mathrm{l}} &= \mathbf{K}_{\mathrm{l1}}\tilde{\mathbf{q}}_{\mathrm{l}} + \mathbf{R}_{\mathrm{l1}}\tilde{\mathbf{q}}_{\mathrm{r}}(t - T_{\mathrm{r}}(t)) + \mathbf{K}_{\mathrm{l2}}\dot{\tilde{\mathbf{q}}}_{\mathrm{l}} + \mathbf{R}_{\mathrm{l2}}\dot{\tilde{\mathbf{q}}}_{\mathrm{r}}(t - T_{\mathrm{r}}(t)) + \underbrace{\mathbf{K}_{\mathrm{l1}}\bar{\mathbf{q}}_{\mathrm{l}} + \mathbf{R}_{\mathrm{l1}}\bar{\mathbf{q}}_{\mathrm{r}} + \mathbf{F}_{\mathrm{op}}}_{\mathbf{0}}, \\
\mathbf{M}_{\mathrm{r}}\ddot{\tilde{\mathbf{q}}}_{\mathrm{r}} + \mathbf{C}_{\mathrm{r}}\dot{\tilde{\mathbf{q}}}_{\mathrm{r}} &= \mathbf{K}_{\mathrm{r1}}\tilde{\mathbf{q}}_{\mathrm{r}} + \mathbf{R}_{\mathrm{r1}}\tilde{\mathbf{q}}_{\mathrm{l}}(t - T_{\mathrm{l}}(t)) + \mathbf{K}_{\mathrm{r2}}\dot{\tilde{\mathbf{q}}}_{\mathrm{r}} + \mathbf{R}_{\mathrm{r2}}\dot{\tilde{\mathbf{q}}}_{\mathrm{l}}(t - T_{\mathrm{l}}(t)) - \mathbf{K}_{\mathrm{e}}\tilde{\mathbf{q}}_{\mathrm{r}} - \mathbf{B}_{\mathrm{e}}\dot{\tilde{\mathbf{q}}}_{\mathrm{r}} \\
&\quad + \underbrace{\mathbf{K}_{\mathrm{r1}}\bar{\mathbf{q}}_{\mathrm{r}} + \mathbf{R}_{\mathrm{r1}}\bar{\mathbf{q}}_{\mathrm{l}} + G\mathbf{F}_{\mathrm{op}}(t - T_{\mathrm{l}}(t)) - \mathbf{K}_{\mathrm{e}}\bar{\mathbf{q}}_{\mathrm{r}}}_{\mathbf{0}}.
\end{aligned}$$

Then the dynamics of a bilateral teleoperation system in a closed loop is given by

$$\begin{aligned}
\mathbf{M}_{\mathrm{l}}\ddot{\tilde{\mathbf{q}}}_{\mathrm{l}} + \mathbf{C}_{\mathrm{l}}\dot{\tilde{\mathbf{q}}}_{\mathrm{l}} &= \mathbf{K}_{\mathrm{l1}}\tilde{\mathbf{q}}_{\mathrm{l}} + \mathbf{R}_{\mathrm{l1}}\tilde{\mathbf{q}}_{\mathrm{r}}(t - T_{\mathrm{r}}(t)) + \mathbf{K}_{\mathrm{l2}}\dot{\tilde{\mathbf{q}}}_{\mathrm{l}} + \mathbf{R}_{\mathrm{l2}}\dot{\tilde{\mathbf{q}}}_{\mathrm{r}}(t - T_{\mathrm{r}}(t)), \\
\mathbf{M}_{\mathrm{r}}\ddot{\tilde{\mathbf{q}}}_{\mathrm{r}} + \mathbf{C}_{\mathrm{r}}\dot{\tilde{\mathbf{q}}}_{\mathrm{r}} &= \mathbf{K}_{\mathrm{r1}}\tilde{\mathbf{q}}_{\mathrm{r}} + \mathbf{R}_{\mathrm{r1}}\tilde{\mathbf{q}}_{\mathrm{l}}(t - T_{\mathrm{l}}(t)) + \mathbf{K}_{\mathrm{r2}}\dot{\tilde{\mathbf{q}}}_{\mathrm{r}} + \mathbf{R}_{\mathrm{r2}}\dot{\tilde{\mathbf{q}}}_{\mathrm{l}}(t - T_{\mathrm{l}}(t)) - \mathbf{K}_{\mathrm{e}}\tilde{\mathbf{q}}_{\mathrm{r}} - \mathbf{B}_{\mathrm{e}}\dot{\tilde{\mathbf{q}}}.
\end{aligned} \tag{11}$$

The following theorem describes the stability properties with respect to the equilibrium points of the closed-loop teleoperation system (11) with the control algorithm given by (6).

Theorem 3.1 *Considering the bilateral teleoperation system given by (11). Setting the control gain as*

$$\begin{aligned}
&\mathbf{K}_{\mathrm{l1}} = -\mathbf{K}, \quad \mathbf{K}_{\mathrm{l2}} = -(2\mathbf{K}_{\mathrm{l}} + \mathbf{K}_{\mathrm{ld}}), \quad \mathbf{K}_{\mathrm{r1}} = -\mathbf{K}, \quad \mathbf{R}_{\mathrm{l2}} = 2\mathbf{K}_{\mathrm{ld}}, \\
&\mathbf{R}_{\mathrm{l1}} = \mathbf{K}, \quad \mathbf{K}_{\mathrm{r2}} = -(2\mathbf{K}_{\mathrm{l}} + \mathbf{K}_{\mathrm{rd}}), \quad \mathbf{R}_{\mathrm{r1}} = \mathbf{K}, \quad \mathbf{R}_{\mathrm{r2}} = 2\mathbf{K}_{\mathrm{rd}},
\end{aligned} \tag{12}$$

where $\mathbf{K}_1$ *and* $\mathbf{K}$ *are constant and positive-definite diagonal matrices, and* $\mathbf{K}_{\mathrm{ld}}$ *and* $\mathbf{K}_{\mathrm{rd}}$ *are positive-definite diagonal matrices given by*

$$\mathbf{K}_{\mathrm{ld}} = \big(1 - \dot{T}_{\mathrm{r}}(t)\big)\mathbf{K}_1, \qquad \mathbf{K}_{\mathrm{rd}} = \big(1 - \dot{T}_{\mathrm{l}}(t)\big)\mathbf{K}_1. \tag{13}$$

If the following is satisfied:

$$\mathbf{K}_1 - \frac{\alpha_1}{2}\mathbf{K} - \frac{T_{\mathrm{l}}^{+^2}}{2\alpha_2}\mathbf{K} > \mathbf{0}, \quad \mathbf{K}_1 - \frac{\alpha_2}{2}\mathbf{K} - \frac{T_{\mathrm{r}}^{+^2}}{2\alpha_1}\mathbf{K} > \mathbf{0}, \tag{14}$$

where α_1, α_2, *and time delay* T_{i}^{+} *for* $i = l, r$ *are scalar constants, then the equilibrium point at the origin is asymptotically stable:*

$$\mathbf{lim}_{t\to\infty}\tilde{\mathbf{q}}_{\mathrm{l}} = \mathbf{lim}_{t\to\infty}\tilde{\mathbf{q}}_{\mathrm{r}} = \mathbf{lim}_{t\to\infty}\dot{\tilde{\mathbf{q}}}_{\mathrm{l}} = \mathbf{lim}_{t\to\infty}\dot{\tilde{\mathbf{q}}}_{\mathrm{r}} = \mathbf{0}.$$

Proof The theorem's proof has five stages, which are listed as follows:

- Stage 1: A Lyapunov–Krasovskii functional $V\left(\dot{\tilde{\mathbf{q}}}_{\mathrm{l}}, \dot{\tilde{\mathbf{q}}}_{\mathrm{r}}, \tilde{\mathbf{q}}_{\mathrm{l}} - \tilde{\mathbf{q}}_{\mathrm{r}}, \tilde{\mathbf{q}}_{\mathrm{r}}\right)$ is put forward to probe the stability of the proposed control scheme.
- Stage 2: Test that the signals $\dot{\tilde{\mathbf{q}}}_{\mathrm{l}}, \dot{\tilde{\mathbf{q}}}_{\mathrm{r}}, \tilde{\mathbf{q}}_{\mathrm{l}} - \tilde{\mathbf{q}}_{\mathrm{r}}, \tilde{\mathbf{q}}_{\mathrm{r}}$ are bounded, i.e., $\left\{\dot{\tilde{\mathbf{q}}}_{\mathrm{l}}, \dot{\tilde{\mathbf{q}}}_{\mathrm{r}}, \tilde{\mathbf{q}}_{\mathrm{l}} - \tilde{\mathbf{q}}_{\mathrm{r}}, \tilde{\mathbf{q}}_{\mathrm{r}}\right\} \in L_\infty$ and $\left\{\dot{\tilde{\mathbf{q}}}_{\mathrm{l}}, \dot{\tilde{\mathbf{q}}}_{\mathrm{r}}\right\} \in L_2$.
- Stage 3: Demonstrate the rate of convergence to zero, i.e., $\lim_{t\to\infty}\dot{\tilde{\mathbf{q}}}_{\mathrm{l}} = \lim_{t\to\infty}\dot{\tilde{\mathbf{q}}}_{\mathrm{r}} = \mathbf{0}$.
- Stage 4: Investigate the acceleration of zero convergence, i.e., $\lim_{t\to\infty}\ddot{\tilde{\mathbf{q}}}_{\mathrm{l}} = \lim_{t\to\infty}\ddot{\tilde{\mathbf{q}}}_{\mathrm{r}} = \mathbf{0}$.
- Stage 5: Finally, asymptotic stability is demonstrated, i.e., $\lim_{t\to\infty}\mathbf{q}_{\mathrm{l}}(t) = \bar{\mathbf{q}}_{\mathrm{l}}$, $\lim_{t\to\infty}\mathbf{q}_{\mathrm{r}}(t) = \bar{\mathbf{q}}_{\mathrm{r}}$.

3.1 Stage 1

For the stability analysis considering a variable time delay, we used a Lyapunov–Krasovskii functional [18–20].

We define V, a positive-definite function as

$$\begin{aligned} V\left(\dot{\tilde{\mathbf{q}}}_{\mathrm{l}}, \dot{\tilde{\mathbf{q}}}_{\mathrm{r}}, \tilde{\mathbf{q}}_{\mathrm{l}}, \tilde{\mathbf{q}}_{\mathrm{r}}\right) &= \frac{1}{2}\dot{\tilde{\mathbf{q}}}_{\mathrm{l}}^{\mathbf{T}}\mathbf{M}_{\mathrm{l}}\dot{\tilde{\mathbf{q}}}_{\mathrm{l}} + \frac{1}{2}\dot{\tilde{\mathbf{q}}}_{\mathrm{r}}^{\mathbf{T}}\mathbf{M}_{\mathrm{r}}\dot{\tilde{\mathbf{q}}}_{\mathrm{r}} + \frac{1}{2}(\tilde{\mathbf{q}}_{\mathrm{l}} - \tilde{\mathbf{q}}_{\mathrm{r}})^{\mathbf{T}}\mathbf{K}(\tilde{\mathbf{q}}_{\mathrm{l}} - \tilde{\mathbf{q}}_{\mathrm{r}}) \\ &\quad + \frac{1}{2}\tilde{\mathbf{q}}_{\mathrm{r}}^{\mathbf{T}}\mathbf{K}_{\mathrm{e}}\tilde{\mathbf{q}}_{\mathrm{r}} + \int_{t-T_{\mathrm{l}}(t)}^{t}\dot{\tilde{\mathbf{q}}}_{\mathrm{l}}^{\mathbf{T}}(\xi)\mathbf{K}_1\dot{\tilde{\mathbf{q}}}_{\mathrm{l}}(\xi)\,\mathrm{d}\xi + \int_{t-T_{\mathrm{r}}(t)}^{t}\dot{\tilde{\mathbf{q}}}_{\mathrm{r}}^{\mathbf{T}}(\xi)\mathbf{K}_1\dot{\tilde{\mathbf{q}}}_{\mathrm{r}}(\xi)\,\mathrm{d}\xi, \end{aligned} \tag{15}$$

where $T_{\mathrm{i}}(t)$ for $i = \mathrm{l}, \mathrm{r}$ is the variable time delay of the communication channel and $\mathbf{K}$, $\mathbf{K}_{\mathrm{e}}$, and $\mathbf{K}_1$ are positive-definite constant diagonal matrices.

3.2 Stage 2

The time derivative of the preceding Lyapunov function along the system trajectories described by (11) is given by

$$\begin{aligned} \dot{V} &= \dot{\tilde{\mathbf{q}}}_{\mathrm{l}}^{\mathbf{T}}\mathbf{M}_{\mathrm{l}}\ddot{\tilde{\mathbf{q}}}_{\mathrm{l}} + \frac{1}{2}\dot{\tilde{\mathbf{q}}}_{\mathrm{l}}^{\mathbf{T}}\dot{\mathbf{M}}_{\mathrm{l}}\dot{\tilde{\mathbf{q}}}_{\mathrm{l}} + \dot{\tilde{\mathbf{q}}}_{\mathrm{r}}^{\mathbf{T}}\mathbf{M}_{\mathrm{r}}\ddot{\tilde{\mathbf{q}}}_{\mathrm{r}} + \frac{1}{2}\dot{\tilde{\mathbf{q}}}_{\mathrm{r}}^{\mathbf{T}}\dot{\mathbf{M}}_{\mathrm{r}}\dot{\tilde{\mathbf{q}}}_{\mathrm{r}} + \left(\dot{\tilde{\mathbf{q}}}_{\mathrm{l}} - \dot{\tilde{\mathbf{q}}}_{\mathrm{r}}\right)^{\mathbf{T}}\mathbf{K}(\tilde{\mathbf{q}}_{\mathrm{l}} - \tilde{\mathbf{q}}_{\mathrm{r}}) + \dot{\tilde{\mathbf{q}}}_{\mathrm{r}}^{\mathbf{T}}\mathbf{K}_{\mathrm{e}}\tilde{\mathbf{q}}_{\mathrm{r}} \\ &\quad + \dot{\tilde{\mathbf{q}}}_{\mathrm{l}}^{\mathbf{T}}\mathbf{K}_1\dot{\tilde{\mathbf{q}}}_{\mathrm{l}} + \dot{\tilde{\mathbf{q}}}_{\mathrm{r}}^{\mathbf{T}}\mathbf{K}_1\dot{\tilde{\mathbf{q}}}_{\mathrm{r}} - \dot{\tilde{\mathbf{q}}}_{\mathrm{l}}^{\mathbf{T}}(t - T_{\mathrm{l}}(t))\mathbf{K}_{\mathrm{rd}}\dot{\tilde{\mathbf{q}}}_{\mathrm{l}}(t - T_{\mathrm{l}}(t)) - \dot{\tilde{\mathbf{q}}}_{\mathrm{r}}^{\mathbf{T}}(t - T_{\mathrm{r}}(t))\mathbf{K}_{\mathrm{ld}}\dot{\tilde{\mathbf{q}}}_{\mathrm{r}}(t - T_{\mathrm{r}}(t)). \end{aligned} \tag{16}$$

Replacing (11), applying the properties of the robot's dynamics [21–23], and simplifying and grouping terms yields

$$\begin{aligned} \dot{V} &= \dot{\tilde{\mathbf{q}}}_{\mathrm{l}}^{\mathbf{T}}(t)\mathbf{K}(\tilde{\mathbf{q}}_{\mathrm{r}}(t - T_{\mathrm{r}}(t)) - \tilde{\mathbf{q}}_{\mathrm{r}}(t)) - \left(\dot{\tilde{\mathbf{q}}}_{\mathrm{r}}(t - T_{\mathrm{r}}(t)) - \dot{\tilde{\mathbf{q}}}_{\mathrm{l}}(t)\right)^{\mathbf{T}}\mathbf{K}_{\mathrm{ld}}\left(\dot{\tilde{\mathbf{q}}}_{\mathrm{r}}(t - T_{\mathrm{r}}(t)) - \dot{\tilde{\mathbf{q}}}_{\mathrm{l}}(t)\right) \\ &\quad + \dot{\tilde{\mathbf{q}}}_{\mathrm{r}}^{\mathbf{T}}(t)\mathbf{K}(\tilde{\mathbf{q}}_{\mathrm{l}}(t - T_{\mathrm{l}}(t)) - \tilde{\mathbf{q}}_{\mathrm{l}}(t)) - \left(\dot{\tilde{\mathbf{q}}}_{\mathrm{l}}(t - T_{\mathrm{l}}(t)) - \dot{\tilde{\mathbf{q}}}_{\mathrm{r}}(t)\right)^{\mathbf{T}}\mathbf{K}_{\mathrm{rd}}\left(\dot{\tilde{\mathbf{q}}}_{\mathrm{l}}(t - T_{\mathrm{l}}(t)) - \dot{\tilde{\mathbf{q}}}_{\mathrm{r}}(t)\right) \end{aligned}$$

$$
\begin{aligned}
&-\dot{\tilde{\mathbf{q}}}_{\mathrm{r}}^{\mathrm{T}}(t)\mathbf{B}_{\mathrm{e}}\dot{\tilde{\mathbf{q}}}_{\mathrm{r}}(t)-\dot{\tilde{\mathbf{q}}}_{\mathrm{l}}^{\mathrm{T}}(t)\mathbf{K}_1\dot{\tilde{\mathbf{q}}}_{\mathrm{l}}(t)-\dot{\tilde{\mathbf{q}}}_{\mathrm{r}}^{\mathrm{T}}(t)\mathbf{K}_1\dot{\tilde{\mathbf{q}}}_{\mathrm{r}}(t)\\
&+\dot{\tilde{\mathbf{q}}}_{\mathrm{l}}^{\mathrm{T}}(\mathbf{K}_{\mathrm{l}1}+\mathbf{K})\tilde{\mathbf{q}}_{\mathrm{l}}+\dot{\tilde{\mathbf{q}}}_{\mathrm{l}}^{\mathrm{T}}(\mathbf{R}_{\mathrm{l}1}-\mathbf{K})\tilde{\mathbf{q}}_{\mathrm{r}}(t-T_{\mathrm{r}}(t))\\
&+\dot{\tilde{\mathbf{q}}}_{\mathrm{l}}^{\mathrm{T}}(\mathbf{R}_{\mathrm{l}2}-2\mathbf{K}_{\mathrm{ld}})\dot{\tilde{\mathbf{q}}}_{\mathrm{r}}(t-T_{\mathrm{r}}(t))+\dot{\tilde{\mathbf{q}}}_{\mathrm{l}}^{\mathrm{T}}(\mathbf{K}_{\mathrm{l}2}+(2\mathbf{K}_1+\mathbf{K}_{\mathrm{ld}}))\dot{\tilde{\mathbf{q}}}_{\mathrm{l}}\\
&+\dot{\tilde{\mathbf{q}}}_{\mathrm{r}}^{\mathrm{T}}(\mathbf{K}_{\mathrm{r}1}+\mathbf{K})\tilde{\mathbf{q}}_{\mathrm{r}}+\dot{\tilde{\mathbf{q}}}_{\mathrm{r}}^{\mathrm{T}}(\mathbf{R}_{\mathrm{r}1}-\mathbf{K})\tilde{\mathbf{q}}_{\mathrm{l}}(t-T_{\mathrm{l}}(t))\\
&+\dot{\tilde{\mathbf{q}}}_{\mathrm{r}}^{\mathrm{T}}(\mathbf{R}_{\mathrm{r}2}-2\mathbf{K}_{\mathrm{rd}})\dot{\tilde{\mathbf{q}}}_{\mathrm{l}}^{\mathrm{T}}(t-T_{\mathrm{l}}(t))+\dot{\tilde{\mathbf{q}}}_{\mathrm{r}}^{\mathrm{T}}(\mathbf{K}_{\mathrm{r}2}+(2\mathbf{K}_1+\mathbf{K}_{\mathrm{rd}}))\dot{\tilde{\mathbf{q}}}_{\mathrm{r}}. \qquad (17)
\end{aligned}
$$

Defining the error signal as

$$
\dot{\mathbf{e}}_{\tilde{\mathbf{q}}_{\mathrm{l}}}=\dot{\tilde{\mathbf{q}}}_{\mathrm{r}}(t-T_{\mathrm{r}}(t))-\dot{\tilde{\mathbf{q}}}_{\mathrm{l}}(t),\quad \dot{\mathbf{e}}_{\tilde{\mathbf{q}}_{\mathrm{r}}}=\dot{\tilde{\mathbf{q}}}_{\mathrm{l}}(t-T_{\mathrm{l}}(t))-\dot{\tilde{\mathbf{q}}}_{\mathrm{r}}(t) \qquad (18)
$$

and substituting (18) and (12) into (17) yields

$$
\begin{aligned}
\dot{V}=&\,\dot{\tilde{\mathbf{q}}}_{\mathrm{l}}\mathbf{K}\big[\tilde{\mathbf{q}}_{\mathrm{r}}(t-T_{\mathrm{r}}(t))-\tilde{\mathbf{q}}_{\mathrm{r}}(t)\big]-\dot{\mathbf{e}}_{\tilde{\mathbf{q}}_{\mathrm{l}}}^{\mathrm{T}}\mathbf{K}_{\mathrm{ld}}\dot{\mathbf{e}}_{\tilde{\mathbf{q}}_{\mathrm{l}}}+\dot{\tilde{\mathbf{q}}}_{\mathrm{r}}^{\mathrm{T}}\mathbf{K}\big[\tilde{\mathbf{q}}_{\mathrm{l}}(t-T_{\mathrm{l}}(t))-\tilde{\mathbf{q}}_{\mathrm{l}}(t)\big]\\
&-\dot{\mathbf{e}}_{\tilde{\mathbf{q}}_{\mathrm{r}}}^{\mathrm{T}}\mathbf{K}_{\mathrm{rd}}\dot{\mathbf{e}}_{\tilde{\mathbf{q}}_{\mathrm{r}}}-\dot{\tilde{\mathbf{q}}}_{\mathrm{r}}^{\mathrm{T}}\mathbf{B}_{\mathrm{e}}\dot{\tilde{\mathbf{q}}}_{\mathrm{r}}-\dot{\tilde{\mathbf{q}}}_{\mathrm{l}}^{\mathrm{T}}\mathbf{K}_1\dot{\tilde{\mathbf{q}}}_{\mathrm{l}}-\dot{\tilde{\mathbf{q}}}_{\mathrm{r}}^{\mathrm{T}}\mathbf{K}_1\dot{\tilde{\mathbf{q}}}_{\mathrm{r}}. \qquad (19)
\end{aligned}
$$

Taking into account that $\tilde{\mathbf{q}}_{\mathrm{i}}(t-T_i(t))-\tilde{\mathbf{q}}_{\mathrm{i}}(t)=-\int_0^{T_i(t)}\dot{\tilde{\mathbf{q}}}_{\mathrm{i}}(t-\sigma)\,\mathrm{d}\sigma$ and substituting this expression into (19), we obtain the following result:

$$
\begin{aligned}
\dot{V}=&-\dot{\mathbf{e}}_{\tilde{\mathbf{q}}_{\mathrm{l}}}^{\mathrm{T}}\mathbf{K}_{\mathrm{ld}}\dot{\mathbf{e}}_{\tilde{\mathbf{q}}_{\mathrm{l}}}-\dot{\mathbf{e}}_{\tilde{\mathbf{q}}_{\mathrm{r}}}^{\mathrm{T}}\mathbf{K}_{\mathrm{rd}}\dot{\mathbf{e}}_{\tilde{\mathbf{q}}_{\mathrm{r}}}-\dot{\tilde{\mathbf{q}}}_{\mathrm{r}}^{\mathrm{T}}\mathbf{B}_{\mathrm{e}}\dot{\tilde{\mathbf{q}}}_{\mathrm{r}}-\dot{\tilde{\mathbf{q}}}_{\mathrm{l}}^{\mathrm{T}}\mathbf{K}_1\dot{\tilde{\mathbf{q}}}_{\mathrm{l}}-\dot{\tilde{\mathbf{q}}}_{\mathrm{r}}^{\mathrm{T}}\mathbf{K}_1\dot{\tilde{\mathbf{q}}}_{\mathrm{r}}\\
&-\dot{\tilde{\mathbf{q}}}_{\mathrm{l}}^{\mathrm{T}}\mathbf{K}\int_0^{T_{\mathrm{r}}(t)}\dot{\tilde{\mathbf{q}}}_{\mathrm{r}}(t-\sigma)\,\mathrm{d}\sigma-\dot{\tilde{\mathbf{q}}}_{\mathrm{r}}^{\mathrm{T}}\mathbf{K}\int_0^{T_{\mathrm{l}}(t)}\dot{\tilde{\mathbf{q}}}_{\mathrm{l}}(t-\sigma)\,\mathrm{d}\sigma, \qquad (20)
\end{aligned}
$$

$$
\begin{aligned}
\int_0^{t_f}\dot{V}\mathrm{d}t=&-\int_0^{t_f}\dot{\mathbf{e}}_{\tilde{\mathbf{q}}_{\mathrm{l}}}^{\mathrm{T}}\mathbf{K}_{\mathrm{ld}}\dot{\mathbf{e}}_{\tilde{\mathbf{q}}_{\mathrm{l}}}\,\mathrm{d}t-\int_0^{t_f}\dot{\mathbf{e}}_{\tilde{\mathbf{q}}_{\mathrm{r}}}^{\mathrm{T}}\mathbf{K}_{\mathrm{rd}}\dot{\mathbf{e}}_{\tilde{\mathbf{q}}_{\mathrm{r}}}\,\mathrm{d}t-\int_0^{t_f}\dot{\tilde{\mathbf{q}}}_{\mathrm{l}}^{\mathrm{T}}\mathbf{K}_1\dot{\tilde{\mathbf{q}}}_{\mathrm{l}}\,\mathrm{d}t-\int_0^{t_f}\dot{\tilde{\mathbf{q}}}_{\mathrm{r}}^{\mathrm{T}}\mathbf{K}_1\dot{\tilde{\mathbf{q}}}_{\mathrm{r}}\,\mathrm{d}t\\
&-\int_0^{t_f}\dot{\tilde{\mathbf{q}}}_{\mathrm{l}}^{\mathrm{T}}\mathbf{K}\int_0^{T_{\mathrm{r}}(t)}\dot{\tilde{\mathbf{q}}}_{\mathrm{r}}(t-\sigma)\,\mathrm{d}\sigma\,\mathrm{d}t-\int_0^{t_f}\dot{\tilde{\mathbf{q}}}_{\mathrm{r}}^{\mathrm{T}}\mathbf{K}\int_0^{T_l(t)}\dot{\tilde{\mathbf{q}}}_{\mathrm{l}}(t-\sigma)\,\mathrm{d}\sigma\,\mathrm{d}t-\int_0^{t_f}\dot{\tilde{\mathbf{q}}}_{\mathrm{r}}^{\mathrm{T}}\mathbf{B}_{\mathrm{e}}\dot{\tilde{\mathbf{q}}}_{\mathrm{r}}\,\mathrm{d}t. \qquad (21)
\end{aligned}
$$

For any vector signals $\mathbf{x},\mathbf{y}\in\mathbf{R}^{\mathbf{n}}$, for a positive-definite diagonal matrix $\mathbf{K}\in\mathbf{R}^{n\times n}$, $\alpha\in\mathbf{R}^{+}$, and for any continuously differentiable functions that have a known upper bound T_{i}^{+} defined by $T_i(t)\le T_i^{+}<\infty$ we have that

$$
-2\int_0^{t_f}\dot{\mathbf{x}}^{\mathrm{T}}\mathbf{K}\int_0^{T_i(t)}\dot{\mathbf{y}}(\mathbf{t}-\boldsymbol{\sigma})\,\mathrm{d}\sigma\,\mathrm{d}t\le\alpha\int_0^{t_f}\dot{\mathbf{x}}^{\mathrm{T}}\mathbf{K}\dot{\mathbf{x}}\,\mathrm{d}t+\frac{T_i^{+2}}{\alpha}\int_0^{t_f}\dot{\mathbf{y}}^{\mathrm{T}}\mathbf{K}\dot{\mathbf{y}}\,\mathrm{d}t. \qquad (22)
$$

Substituting (22) into (21) yields

$$
\begin{aligned}
\int_0^{t_f}\dot{V}\,\mathrm{d}t\le&-\int_0^{t_f}\dot{\mathbf{e}}_{\tilde{\mathbf{q}}_{\mathrm{l}}}^{\mathrm{T}}\mathbf{K}_{\mathrm{ld}}\dot{\mathbf{e}}_{\tilde{\mathbf{q}}_{\mathrm{l}}}\,\mathrm{d}t-\int_0^{t_f}\dot{\mathbf{e}}_{\tilde{\mathbf{q}}_{\mathrm{r}}}^{\mathrm{T}}\mathbf{K}_{\mathrm{rd}}\dot{\mathbf{e}}_{\tilde{\mathbf{q}}_{\mathrm{r}}}\,\mathrm{d}t-\int_0^{t_f}\dot{\tilde{\mathbf{q}}}_{\mathrm{l}}^{\mathrm{T}}\mathbf{K}_1\dot{\tilde{\mathbf{q}}}_{\mathrm{l}}\,\mathrm{d}t-\int_0^{t_f}\dot{\tilde{\mathbf{q}}}_{\mathrm{r}}^{\mathrm{T}}\mathbf{K}_1\dot{\tilde{\mathbf{q}}}_{\mathrm{r}}\,\mathrm{d}t-\int_0^{t_f}\dot{\tilde{\mathbf{q}}}_{\mathrm{r}}^{\mathrm{T}}\mathbf{B}_{\mathrm{e}}\dot{\tilde{\mathbf{q}}}_{\mathrm{r}}\,\mathrm{d}t\\
&+\frac{\alpha_1}{2}\int_0^{t_f}\dot{\tilde{\mathbf{q}}}_{\mathrm{l}}^{\mathrm{T}}\mathbf{K}\dot{\tilde{\mathbf{q}}}_{\mathrm{l}}\,\mathrm{d}t+\frac{T_r^{+2}}{2\alpha_1}\int_0^{t_f}\dot{\tilde{\mathbf{q}}}_{\mathrm{r}}^{\mathrm{T}}\mathbf{K}\dot{\tilde{\mathbf{q}}}_{\mathrm{r}}\,\mathrm{d}t+\frac{\alpha_2}{2}\int_0^{t_f}\dot{\tilde{\mathbf{q}}}_{\mathrm{r}}^{\mathrm{T}}\mathbf{K}\dot{\tilde{\mathbf{q}}}_{\mathrm{r}}\,\mathrm{d}t+\frac{T_l^{+2}}{2\alpha_2}\int_0^{t_f}\dot{\tilde{\mathbf{q}}}_{\mathrm{l}}^{\mathrm{T}}\mathbf{K}\dot{\tilde{\mathbf{q}}}_{\mathrm{l}}\,\mathrm{d}t. \qquad (23)
\end{aligned}
$$

Therefore, integral inequality (23) is reduced to

$$\int_0^{t_f} \dot{V}\,\mathrm{d}t \leq -\mu(\mathbf{K}_{\mathrm{ld}})\left\|\dot{\mathbf{e}}_{\tilde{\mathbf{q}}_\mathrm{l}}\right\|_2^2 - \mu(\mathbf{K}_{\mathrm{rd}})\left\|\dot{\mathbf{e}}_{\tilde{\mathbf{q}}_\mathrm{r}}\right\|_2^2 - \mu(\mathbf{B}_\mathrm{e})\left\|\dot{\tilde{\mathbf{q}}}_\mathrm{r}\right\|_2^2$$
$$-\mu\left(\mathbf{K}_1 - \frac{\alpha_1}{2}\mathbf{K} - \frac{T_l^{+2}}{2\alpha_2}\mathbf{K}\right)\left\|\dot{\tilde{\mathbf{q}}}_\mathrm{l}\right\|_2^2 - \mu\left(\mathbf{K}_1 - \frac{\alpha_2}{2}\mathbf{K} - \frac{T_r^{+2}}{2\alpha_1}\mathbf{K}\right)\left\|\dot{\tilde{\mathbf{q}}}_\mathrm{r}\right\|_2^2, \tag{24}$$

where $\mu(\mathbf{A})$ specifies the smallest eigenvalue of $\mathbf{A}$, and the notation $\|\cdot\|_2$ specifies the L_2 norm of a signal in the interval $[0, t_f]$.

Since $\mathbf{B}_\mathrm{e}$, $\mathbf{K}_{\mathrm{ld}}$, and $\mathbf{K}_{\mathrm{rd}}$ are positive-definite matrices, from (24), $\int_0^{t_f} \dot{V}\,\mathrm{d}t \leq 0$, if the relations in (25) are satisfied:

$$\mathbf{K}_1 - \frac{\alpha_1}{2}\mathbf{K} - \frac{T_l^{+2}}{2\alpha_2}\mathbf{K} > 0, \qquad \mathbf{K}_1 - \frac{\alpha_2}{2}\mathbf{K} - \frac{T_r^{+2}}{2\alpha_1}\mathbf{K} > 0. \tag{25}$$

Considering that $\lim_{t_f\to\infty} \int_0^{\infty} \dot{V}\mathrm{d}t \leq 0$, it is possible to conclude that the signals $\left\{\dot{\tilde{\mathbf{q}}}_\mathrm{l}, \dot{\tilde{\mathbf{q}}}_\mathrm{r}, \tilde{\mathbf{q}}_\mathrm{r} - \tilde{\mathbf{q}}_\mathrm{l}, \tilde{\mathbf{q}}_\mathrm{r}\right\} \in L_\infty$ and $\left\{\dot{\tilde{\mathbf{q}}}_\mathrm{l}, \dot{\tilde{\mathbf{q}}}_\mathrm{r}, \dot{\mathbf{e}}_{\tilde{\mathbf{q}}_\mathrm{l}}, \dot{\mathbf{e}}_{\tilde{\mathbf{q}}_\mathrm{r}}\right\} \in L_2$.

3.3 Stage 3: Rate of convergence to zero

We write (11) as

$$\ddot{\tilde{\mathbf{q}}}_\mathrm{l} = -\mathbf{M}_l^{-1}\left[\mathbf{C}_\mathrm{l}\dot{\tilde{\mathbf{q}}}_\mathrm{l} - \mathbf{K}_{\mathrm{l}1}\tilde{\mathbf{q}}_\mathrm{l} - \mathbf{R}_{\mathrm{l}1}\tilde{\mathbf{q}}_\mathrm{r}(t - T_\mathrm{r}(t)) - \mathbf{K}_{\mathrm{l}2}\dot{\tilde{\mathbf{q}}}_\mathrm{l} - \mathbf{R}_{\mathrm{l}2}\dot{\tilde{\mathbf{q}}}_\mathrm{r}(t - T_\mathrm{r}(t))\right],$$
$$\ddot{\tilde{\mathbf{q}}}_\mathrm{r} = -\mathbf{M}_r^{-1}\left[\mathbf{C}_\mathrm{r}\dot{\tilde{\mathbf{q}}}_\mathrm{r} - \mathbf{K}_{\mathrm{r}1}\tilde{\mathbf{q}}_\mathrm{r} - \mathbf{R}_{\mathrm{r}1}\tilde{\mathbf{q}}_\mathrm{l}(t - T_\mathrm{l}(t)) - \mathbf{K}_{\mathrm{r}2}\dot{\tilde{\mathbf{q}}}_\mathrm{r} - \mathbf{R}_{\mathrm{r}2}\dot{\tilde{\mathbf{q}}}_\mathrm{l}(t - T_\mathrm{l}(t)) + \mathbf{K}_\mathrm{e}\tilde{\mathbf{q}}_\mathrm{r} + \mathbf{B}_\mathrm{e}\dot{\tilde{\mathbf{q}}}_\mathrm{r}\right]. \tag{26}$$

It has already been proven that $\dot{\tilde{\mathbf{q}}}_\mathrm{l}, \dot{\tilde{\mathbf{q}}}_\mathrm{r} \in L_2$ and $\left\{\dot{\tilde{\mathbf{q}}}_\mathrm{l}, \dot{\tilde{\mathbf{q}}}_\mathrm{r}, \tilde{\mathbf{q}}_\mathrm{r} - \tilde{\mathbf{q}}_\mathrm{l}, \tilde{\mathbf{q}}_\mathrm{r}\right\} \in L_\infty$. Now it is necessary to prove that $\tilde{\mathbf{q}}_\mathrm{l} - \tilde{\mathbf{q}}_\mathrm{r}(t - T_\mathrm{r}(t)) \in L_\infty$.

We write $\tilde{\mathbf{q}}_\mathrm{l} - \tilde{\mathbf{q}}_\mathrm{r}(t - T_\mathrm{r}(t))$ as

$$\tilde{\mathbf{q}}_\mathrm{l} - \tilde{\mathbf{q}}_\mathrm{r}(t - T_\mathrm{r}(t)) = \tilde{\mathbf{q}}_\mathrm{l} - \tilde{\mathbf{q}}_\mathrm{r} + \tilde{\mathbf{q}}_\mathrm{r} - \tilde{\mathbf{q}}_\mathrm{r}(t - T_\mathrm{r}(t)). \tag{27}$$

Since it is known that $\tilde{\mathbf{q}}_\mathrm{l} - \tilde{\mathbf{q}}_\mathrm{r} \in L_\infty$, the signal $\tilde{\mathbf{q}}_\mathrm{r} - \tilde{\mathbf{q}}_\mathrm{r}(t - T_\mathrm{r}(t))$ must be analyzed. Using Schwartz's inequality we obtain

$$\tilde{\mathbf{q}}_\mathrm{r} - \tilde{\mathbf{q}}_\mathrm{r}(t - T_\mathrm{r}(t)) = \int_0^{T_\mathrm{r}(t)} \dot{\tilde{\mathbf{q}}}_\mathrm{r}(t - \sigma)\mathrm{d}\sigma \leq T_\mathrm{r}^{+1/2}\left\|\dot{\tilde{\mathbf{q}}}_\mathrm{r}\right\|_2 \in L_\infty. \tag{28}$$

Using (28) and $\tilde{\mathbf{q}}_\mathrm{l} - \tilde{\mathbf{q}}_\mathrm{r} \in L_\infty$ in (27), it was concluded that $\tilde{\mathbf{q}}_\mathrm{l} - \tilde{\mathbf{q}}_\mathrm{r}(t - T_\mathrm{r}(t)) \in L_\infty$. In the same way, it was proven that $\tilde{\mathbf{q}}_\mathrm{r} - \tilde{\mathbf{q}}_\mathrm{l}(t - T_\mathrm{l}(t)) \in L_\infty$.

From (26), taking into account the basic properties (inertia matrix and Coriolis matrix properties) of the dynamic model for robots [21–23], the fact that $\left\{\dot{\tilde{\mathbf{q}}}_\mathrm{l}, \dot{\tilde{\mathbf{q}}}_\mathrm{r}, \tilde{\mathbf{q}}_\mathrm{l} - \tilde{\mathbf{q}}_\mathrm{r}, \tilde{\mathbf{q}}_\mathrm{r} - \tilde{\mathbf{q}}_\mathrm{l}(t - T_\mathrm{l}(t)), \tilde{\mathbf{q}}_\mathrm{l} - \tilde{\mathbf{q}}_\mathrm{r}(t - T_\mathrm{r}(t))\right\} \in L_\infty$ ensures that $\left\{\dot{\tilde{\mathbf{q}}}_\mathrm{l}, \dot{\tilde{\mathbf{q}}}_\mathrm{r}\right\} \in L_\infty$ are uniformly continuous [24]. Also, because $\left\{\dot{\tilde{\mathbf{q}}}_\mathrm{l}, \dot{\tilde{\mathbf{q}}}_\mathrm{r}\right\} \in L_2$, using Barbalat's lemma [25], it can be seen that

$$\lim_{t\to\infty} \dot{\tilde{\mathbf{q}}}_\mathrm{l} = \lim_{t\to\infty} \dot{\tilde{\mathbf{q}}}_\mathrm{r} = \lim_{t\to\infty} \dot{\mathbf{e}}_{\tilde{\mathbf{q}}_\mathrm{l}} = \lim_{t\to\infty} \dot{\mathbf{e}}_{\tilde{\mathbf{q}}_\mathrm{r}} = \mathbf{0}.$$

3.4 Stage 4: Acceleration of zero convergence

Analyzing the time derivative of (26), and by dynamical properties of robots, $\left\{\dot{\tilde{\mathbf{q}}}_\mathrm{l}, \dot{\tilde{\mathbf{q}}}_\mathrm{r}, \tilde{\mathbf{q}}_\mathrm{l} - \tilde{\mathbf{q}}_\mathrm{r}, \tilde{\mathbf{q}}_\mathrm{r} - \tilde{\mathbf{q}}_\mathrm{l}(t - T_\mathrm{l}(t)), \tilde{\mathbf{q}}_\mathrm{l} - \tilde{\mathbf{q}}_\mathrm{r}(t - T_\mathrm{r}(t))\right\} \in L_\infty$ and $\left\{\dot{\tilde{\mathbf{q}}}_\mathrm{l}, \dot{\tilde{\mathbf{q}}}_\mathrm{r}\right\} \in L_2$ ensure that $\left\{\ddot{\tilde{\mathbf{q}}}_\mathrm{l}, \ddot{\tilde{\mathbf{q}}}_\mathrm{r}\right\} \in L_\infty$. Then the signals $\left\{\ddot{\tilde{\mathbf{q}}}_\mathrm{l}, \ddot{\tilde{\mathbf{q}}}_\mathrm{r}\right\}$ are uniformly continuous [24]. Signal continuity implies that the integral exists and is bounded by

$$\int_0^t \ddot{\tilde{\mathbf{q}}}_\mathrm{i}(\sigma)\,\mathrm{d}\sigma = \dot{\tilde{\mathbf{q}}}_\mathrm{i}(\sigma) - \dot{\tilde{\mathbf{q}}}_\mathrm{i}(0).$$

When $t \to \infty$ and, shown earlier, $\lim_{t\to\infty} \dot{\tilde{\mathbf{q}}}_\mathrm{l} = \lim_{t\to\infty} \dot{\tilde{\mathbf{q}}}_\mathrm{r} = \mathbf{0}$, we obtain

$$\int_0^\infty \ddot{\tilde{\mathbf{q}}}_\mathrm{i}(\sigma)\,\mathrm{d}\sigma = -\dot{\tilde{\mathbf{q}}}_\mathrm{i}(0).$$

Then the signal is bounded. By Barbalat's lemma [26] it can be proven that

$$\lim_{t\to\infty} \ddot{\tilde{\mathbf{q}}}_\mathrm{l} = \lim_{t\to\infty} \ddot{\tilde{\mathbf{q}}}_\mathrm{r} = 0.$$

3.5 Stage 5: Asymptotic stability

Because the velocity and acceleration signals will go to zero, and using the control gains given by (12) in (11), the following results hold:

$$\lim_{t\to\infty} \|\tilde{\mathbf{q}}_\mathrm{r}(t - T_\mathrm{r}(t)) - \tilde{\mathbf{q}}_\mathrm{l}\| = \mathbf{0}, \qquad \lim_{t\to\infty} \|\tilde{\mathbf{q}}_\mathrm{l}(t - T_\mathrm{l}(t)) - \tilde{\mathbf{q}}_\mathrm{r}\| = \mathbf{K}^{-1}\mathbf{K}_\mathrm{e} \lim_{t\to\infty} \tilde{\mathbf{q}}_\mathrm{r}. \tag{29}$$

Taking into account that $\tilde{\mathbf{q}}_\mathrm{l}(t - T_\mathrm{l}(t)) = \tilde{\mathbf{q}}_\mathrm{l}(t) - \int_{t-T_\mathrm{l}(t)}^t \dot{\tilde{\mathbf{q}}}_\mathrm{l}(t)\mathrm{d}t$, and $\tilde{\mathbf{q}}_\mathrm{r}(t - T_\mathrm{r}(t)) = \tilde{\mathbf{q}}_\mathrm{r}(t) - \int_{t-T_\mathrm{r}(t)}^t \dot{\tilde{\mathbf{q}}}_\mathrm{r}(t)\mathrm{d}t$ and that $\lim_{t\to\infty} \dot{\tilde{\mathbf{q}}}_\mathrm{l} = \lim_{t\to\infty} \dot{\tilde{\mathbf{q}}}_\mathrm{r} = \mathbf{0}$, we obtain

$$\lim_{t\to\infty} \|\tilde{\mathbf{q}}_\mathrm{r}(t) - \tilde{\mathbf{q}}_\mathrm{l}(t)\| = \mathbf{0}, \qquad \lim_{t\to\infty} \|\tilde{\mathbf{q}}_\mathrm{l}(t) - \tilde{\mathbf{q}}_\mathrm{r}(t)\| = \mathbf{K}^{-1}\mathbf{K}_\mathrm{e} \lim_{t\to\infty} \tilde{\mathbf{q}}_\mathrm{r}(t). \tag{30}$$

The preceding equations imply that $\lim_{t\to\infty} \tilde{\mathbf{q}}_\mathrm{l}(t) = \lim_{t\to\infty} \tilde{\mathbf{q}}_\mathrm{r}(t) = \mathbf{0}$.

Therefore, the origin of the system $\left\{\dot{\tilde{\mathbf{q}}}_\mathrm{l}, \dot{\tilde{\mathbf{q}}}_\mathrm{r}, \tilde{\mathbf{q}}_\mathrm{l}, \tilde{\mathbf{q}}_\mathrm{r}\right\}$ is asymptotically stable, and $\lim_{t\to\infty} \mathbf{q}_\mathrm{l}(t) = \bar{\mathbf{q}}_\mathrm{l}$, $\lim_{t\to\infty} \mathbf{q}_\mathrm{r}(t) = \bar{\mathbf{q}}_\mathrm{r}$.

This guarantees the stability of the teleoperation system.

In the following subsection, force reflection and position coordination abilities will be analyzed.

3.6 Static force reflection

Transparency refers to the degree of correspondence between the impedance perceived by the operator and the impedance of the environment. Along with stability, transparency is another important objective of the design of a bilateral teleoperation system.

In steady state, consider the nonlinear teleoperator system described by (5) and the control law given by (6) for the range of control given by (14). This results in the following expression:

$$\mathbf{0} = \mathbf{F}_\mathrm{op} + \mathbf{K}_\mathrm{l1}\bar{\mathbf{q}}_\mathrm{l} + \mathbf{R}_\mathrm{l1}\bar{\mathbf{q}}_\mathrm{r}, \qquad \mathbf{0} = -\mathbf{F}_\mathrm{e} + \mathbf{K}_\mathrm{r1}\bar{\mathbf{q}}_\mathrm{r} + \mathbf{R}_\mathrm{r1}\bar{\mathbf{q}}_\mathrm{l} + G\mathbf{F}_\mathrm{op}.$$

From (12) we obtain

$$\mathbf{F}_\mathrm{op} = \mathbf{K}(\bar{\mathbf{q}}_\mathrm{l} - \bar{\mathbf{q}}_\mathrm{r}), \tag{31}$$

$$\mathbf{0} = -\mathbf{F}_\mathrm{e} + \mathbf{K}(\bar{\mathbf{q}}_\mathrm{l} - \bar{\mathbf{q}}_\mathrm{r}) + G\mathbf{F}_\mathrm{op}. \tag{32}$$

Equations (31) and (32) imply that the static contact force in the remote site is transmitted in a form that is proportional to the human operator on the local side. This can be expressed by

$$\mathbf{F}_{\mathrm{op}} = \frac{\mathbf{F}_{\mathrm{e}}}{1+G}. \tag{33}$$

3.7 Local–remote manipulator position coordination

In cases where the human operator does not move the local manipulator and the remote manipulator does not touch anything, i.e., $\mathbf{F}_{\mathrm{op}} = \mathbf{F}_{\mathrm{e}} = \mathbf{0}$, in steady state, (31) and (32) can be written as $\bar{\mathbf{q}}_{\mathrm{l}} - \bar{\mathbf{q}}_{\mathrm{r}} = \mathbf{0}$, which implies that the equilibrium points of the local and remote manipulators are identical. Then the position coordination error $\tilde{\mathbf{q}}(t) = \mathbf{q}_{\mathrm{l}}(t) - \mathbf{q}_{\mathrm{r}}(t)$ approaches zero as $\lim_{t\to\infty}\tilde{\mathbf{q}}(t) = \lim_{t\to\infty}(\mathbf{q}_{\mathrm{l}}(t) - \mathbf{q}_{\mathrm{r}}(t)) = 0$.

Therefore, there is position coordination between the local and remote manipulators.

4 Simulation results

Figure 3 shows the basic design of the teleoperation system that was used as a model for our simulations. This model was used to simulate the performance of the proposed control strategy. The simulations are carried out using MATLAB and Simulink. For the local side we use a model of a PHANTOM Omni from SensAble Technologies. For the remote side we use a model of a 3-DOF planar serial manipulator. The parameters for both correspond to the experimental test bed to be presented in the next section. The models of local and remote robots are represented in the form given by (1).

The authors employed the Internet's UDP in the communication channel. UDP is commonly applied to the transmission of low-level commands. In this case, the commands relate to low-level control of robot movements, which demand different network requirements.

It is considered that the human operator applies a constant force on the local manipulator, and the remote manipulator interaction with the environment is modeled as a passive mass spring system.

In this simulation the static model of joint friction was considered in the model $\mathbf{f}(\dot{\mathbf{q}}) \in \mathbf{R}^3$. See [21] for details.

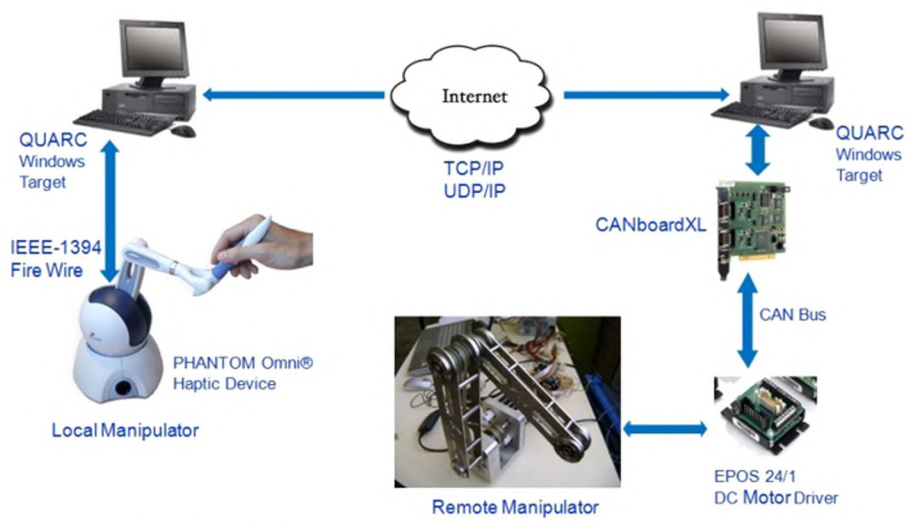

Fig. 3 Schematic model of teleoperation system

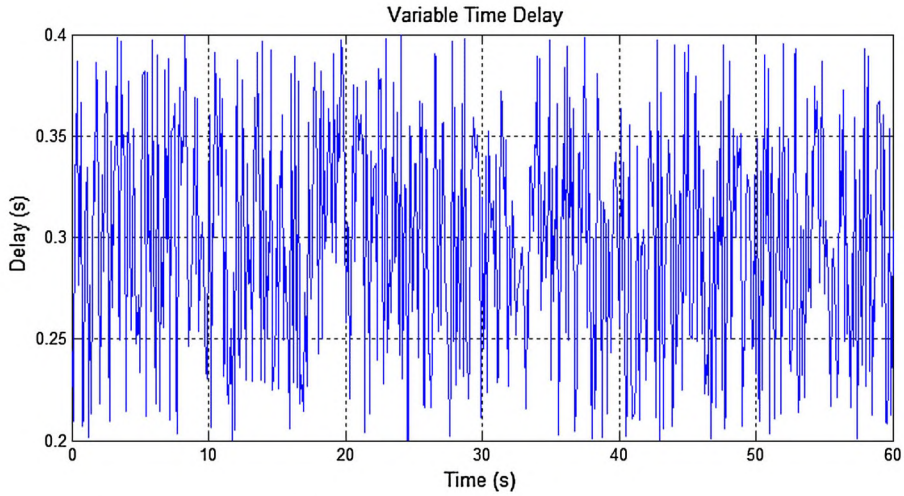

Fig. 4 The variable time delay ranges from 0 to 60 s

Fig. 5 Force (Nm) applied by human operator

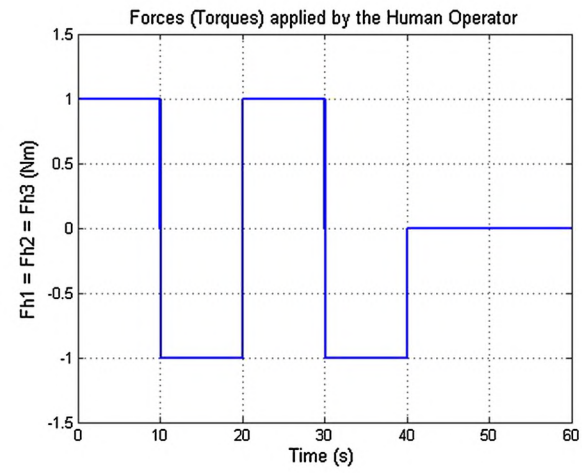

For the simulation, it is assumed that the time delay in both directions has the same value, that is, $T_{\mathrm{r}}^{+} = T_{\mathrm{l}}^{+} = 0.45\,s$. Hence, the upper bound of the round-trip delay in communication is $T_{lr}^{+} = 0.9\,\mathrm{s}$. Figure 4 shows the time delay used in the simulations. The force (torque) applied by the human operator is shown in Fig. 5.

4.1 Gain parameters

Letting $\alpha_1 = T_{\mathrm{r}}^{+}$, $\alpha_2 = T_{\mathrm{l}}^{+}$, $\left|\dot{T}_i(t)\right| = \dot{T}_{\max} = 0.8$, the gains $\mathbf{K}$ and $\mathbf{K}_1$ are calculated using relation (14) by

$$\mathbf{K}_1 = \begin{pmatrix} 40 & 0 & 0 \\ 0 & 30 & 0 \\ 0 & 0 & 10 \end{pmatrix}, \quad \mathbf{K} = \begin{pmatrix} 80 & 0 & 0 \\ 0 & 60 & 0 \\ 0 & 0 & 20 \end{pmatrix}.$$

Then the values for the controller's gains are computed using (12) and (13). In the simulation results it is assumed that $G = 1$.

Two different kinds of simulation were carried out and are detailed in this section:

- Remote robot moves freely, that is, it follows the references given by the human operator without obstacles in the environment.

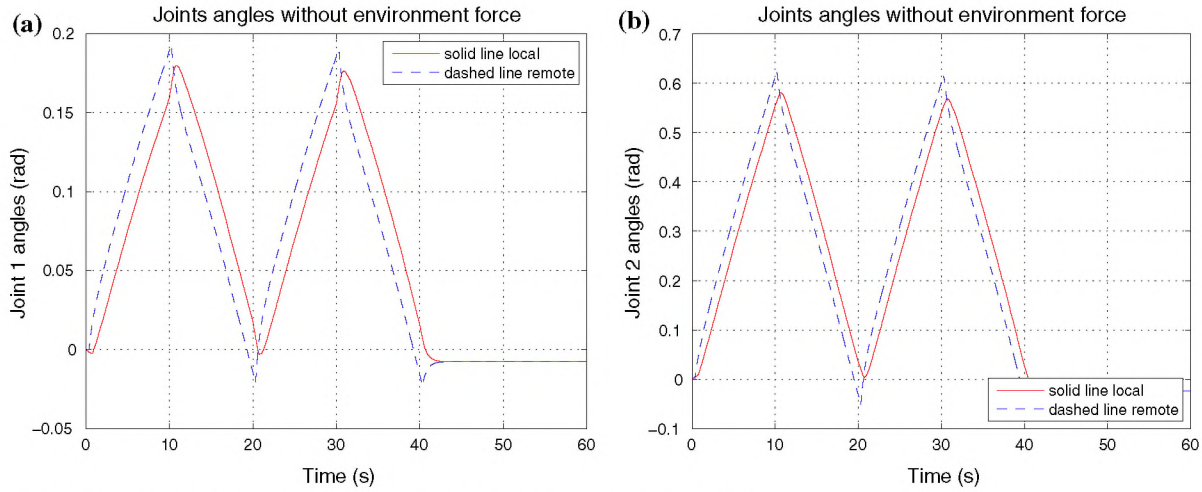

Fig. 6 Angular positions of local and remote manipulators: **a** Joint 1 and **b** Joint 2

- Remote robot must avoid obstacles while human operator sends commands through local robot; then it is necessary to send information to local site (perception of structured environment).

4.2 Case A: Without interaction with environment

Figure 6 shows the simulation results for the case where the remote manipulator does not interact with the environment, i.e., interaction force is zero. It can be observed that good tracking performance can be obtained using the proposed control scheme. The joint angles of the remote manipulator (dashed line) accurately track those of the local manipulator (solid line). When the operator force is zero, at $t = 40\,\mathrm{s}$, the position coordination error $\tilde{\mathbf{q}}(t) = \mathbf{q}_\mathrm{l}(t) - \mathbf{q}_\mathrm{r}(t)$ tends to zero and the equilibrium points of the positions of the local and remote manipulators $\bar{\mathbf{q}}_\mathrm{l}$ and $\bar{\mathbf{q}}_\mathrm{r}$ are identical.

The stability of the teleoperator in a closed loop with the controllers in this scheme (6) was established in Theorem 3.1. The controller guarantees a stable behavior under variable time delays and ensures position tracking.

4.3 Case B: Interaction with environment

To assess the stability of the system when remote manipulator interact with environment, the simulation considered a soft environment modeled by means of a spring–damper system, with the spring and damper gains given as

$$\mathbf{K}_\mathrm{e} = \begin{pmatrix} 25 & 0 & 0 \\ 0 & 25 & 0 \\ 0 & 0 & 25 \end{pmatrix} \mathrm{N/m}, \quad \mathbf{B}_\mathrm{e} = \begin{pmatrix} 1 & 0 & 0 \\ 0 & 1 & 0 \\ 0 & 0 & 1 \end{pmatrix} \mathrm{N\,s/m}.$$

Figure 7 shows the positions of joints for the local and remote manipulators.

When the remote manipulator does not interact with the environment (0–2 and 8–60 s), position coordination of the local and remote manipulator position is achieved.

5 Experimental results

This section presents the experimental performance results of the proposed controller under variable time delay.

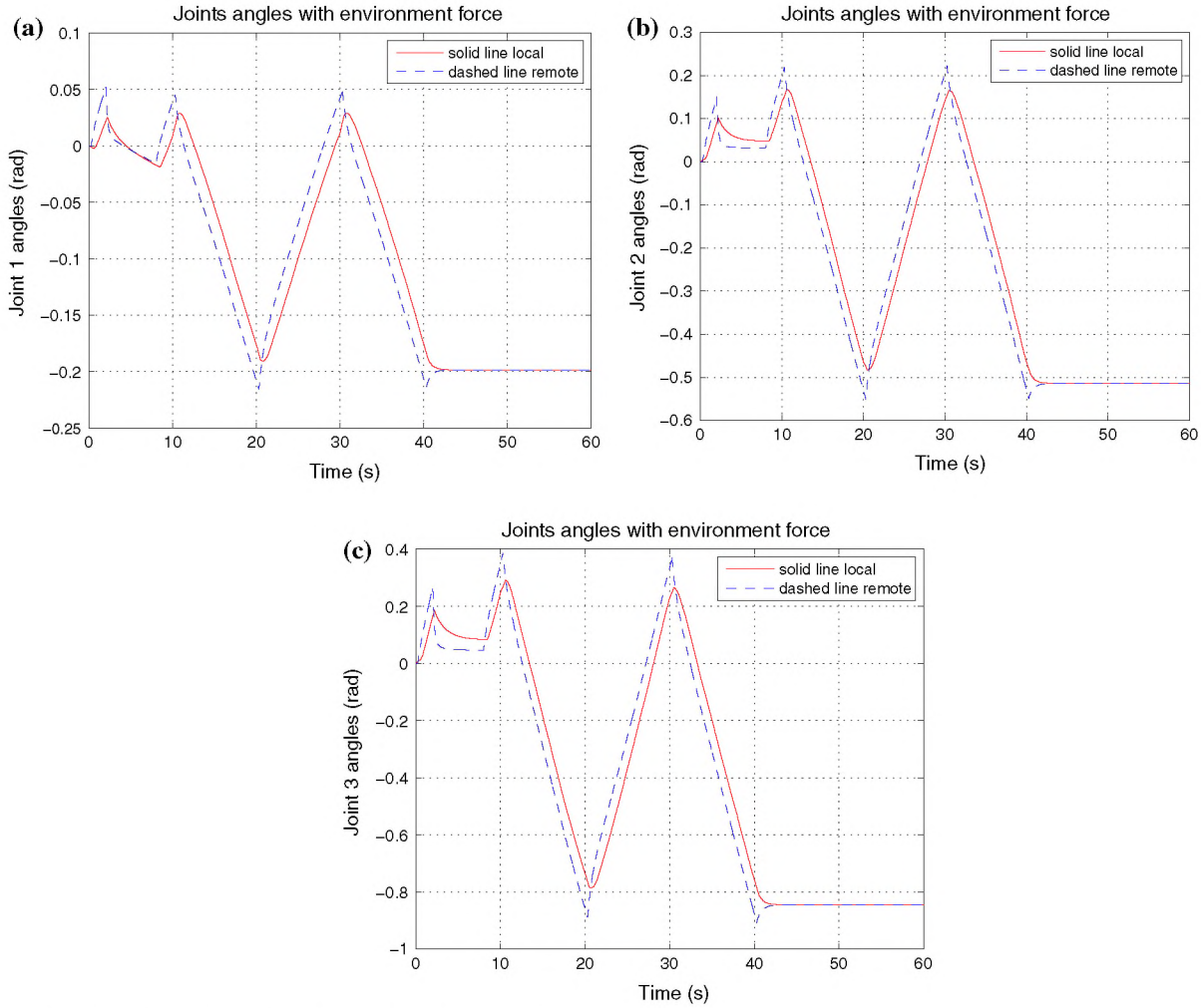

Fig. 7 Angular position of local and remote manipulators: **a** Joint 1, **b** Joint 2, and **c** Joint

Figure 8 shows a photograph of the experimental test bed. The local side consists of a PHANTOM Omni from SensAble Technologies, which is a PC-based six-revolute-joint arm. On the remote manipulator side is placed a 3-DOF planar serial manipulator.

The host and remote computers implement the state convergence control scheme (6) under MATLAB/Simulink using QUARC and Simulink Real-Time Windows Target software running on a Windows XP-based PC. The connection between the two machines running the tasks is implemented using a classic client/server data exchange that uses UDP, similar to the simulation setup.

This local–remote bilateral teleoperation structure allows a human operator to drive the remote manipulator by interacting with a local manipulator, the PHANTOM Omni haptic device [27].

The experiment was carried out for the case where the remote manipulator does not interact with the environment, i.e., the interaction force is zero.

Figure 9 shows that the proposed controller ensures asymptotically stable behavior of the teleoperation system. It also demonstrates that the position of the remote manipulator tracks the local manipulator position. The experimental results validate the theoretical analysis developed in Sect. 3 and the simulation results that were presented in Sect. 4, which show that the equilibrium point at the origin is asymptotically stable. Furthermore, Fig. 10 shows that when

Fig. 8 Experimental test bed

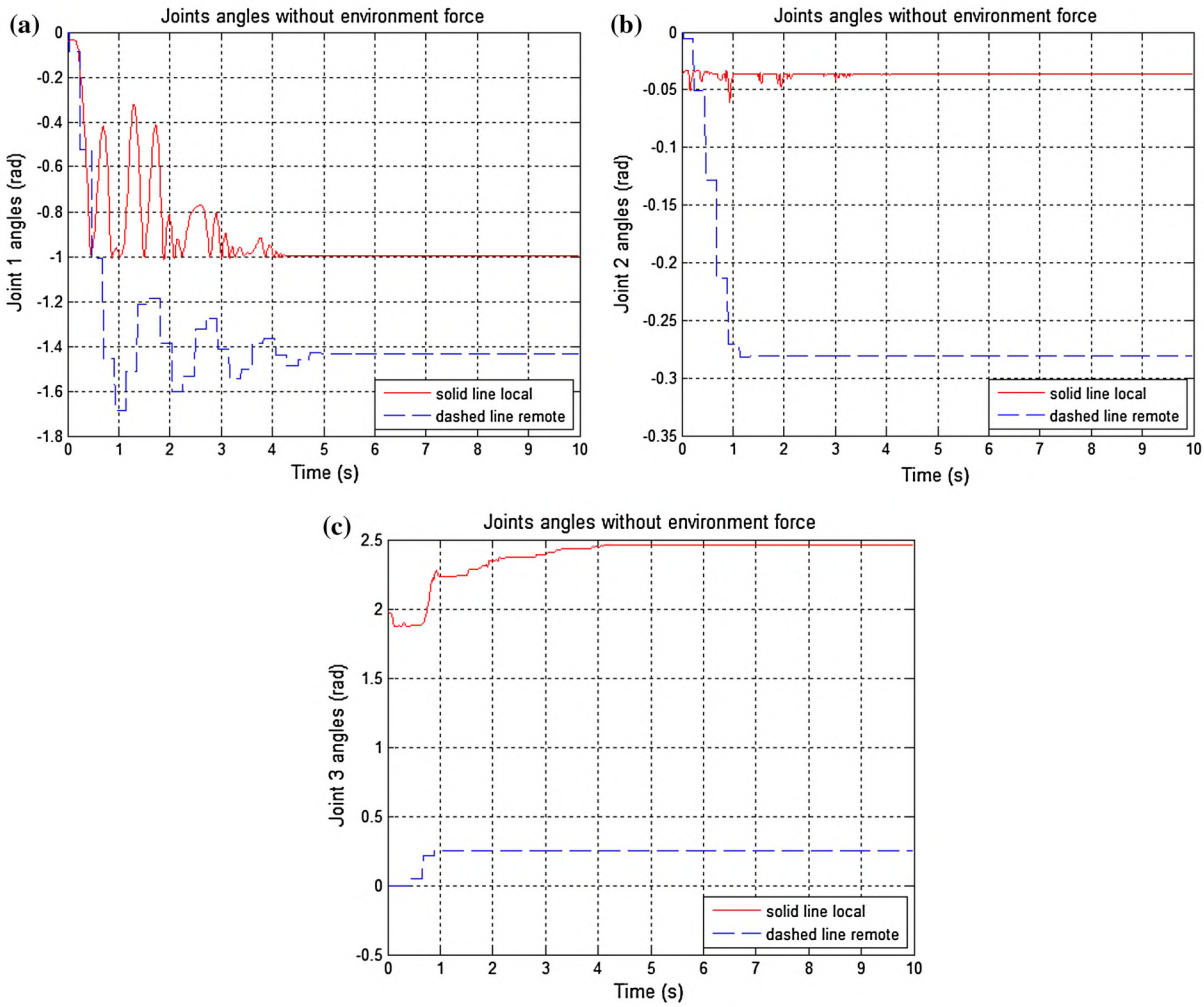

Fig. 9 Angular position of local and remote manipulators: **a** Joint 1, **b** Joint 2, **c** Joint 3

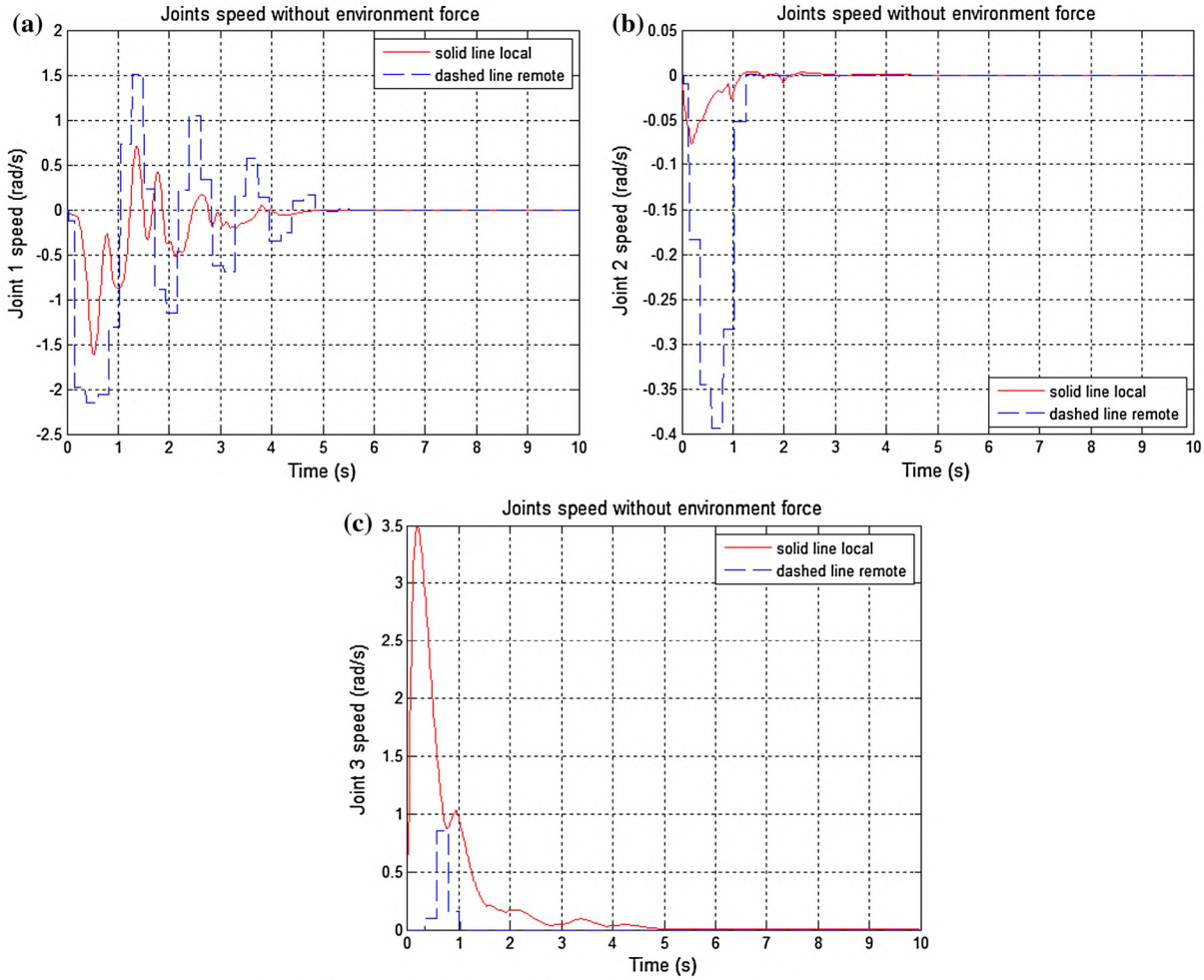

Fig. 10 Angular velocity of local and remote manipulators: **a** Joint 1, **b** Joint 2, **c** Joint 3

the operator ceases to apply force to the local manipulator and the remote manipulator is allowed to move freely, the proposed controller ensures velocity convergence to zero of each of the joints of both the local and remote manipulators. This result was predicted in the theoretical analysis developed in Sect. 3. We consider G = 1 and the gain matrix values used for the control scheme in (6) are given by:

$$\mathbf{K}_{l1} = \begin{pmatrix} -0.45 & 0 & 0 \\ 0 & -0.2 & 0 \\ 0 & 0 & -0.05 \end{pmatrix}, \quad \mathbf{K}_{l2} = \begin{pmatrix} -0.6075 & 0 & 0 \\ 0 & -0.2700 & 0 \\ 0 & 0 & -0.0675 \end{pmatrix},$$

$$\mathbf{R}_{l1} = \begin{pmatrix} 0.045 & 0 & 0 \\ 0 & 0.20 & 0 \\ 0 & 0 & 0.05 \end{pmatrix}, \quad \mathbf{R}_{l2} = \begin{pmatrix} 0.315 & 0 & 0 \\ 0 & 0.140 & 0 \\ 0 & 0 & 0.035 \end{pmatrix},$$

$$\mathbf{K}_{r1} = \begin{pmatrix} -0.45 & 0 & 0 \\ 0 & -0.2 & 0 \\ 0 & 0 & -0.05 \end{pmatrix}, \quad \mathbf{K}_{r2} = \begin{pmatrix} -0.6075 & 0 & 0 \\ 0 & -0.2700 & 0 \\ 0 & 0 & -0.0675 \end{pmatrix},$$

$$\mathbf{R}_{r1} = \begin{pmatrix} 0.045 & 0 & 0 \\ 0 & 0.20 & 0 \\ 0 & 0 & 0.05 \end{pmatrix}, \quad \mathbf{R}_{r2} = \begin{pmatrix} 0.315 & 0 & 0 \\ 0 & 0.140 & 0 \\ 0 & 0 & 0.035 \end{pmatrix}.$$

6 Conclusions

In this paper we have analyzed a novel control scheme based on state convergence for nonlinear, bilateral teleoperation systems of n-DOF variable time delays from both theoretical and experimental points of view. Taking into account time-varying communication delay and possible data-packet dropout, it was demonstrated that the proposed control scheme guarantees the stability of the overall system if suitable control gains are used.

In a teleoperation system, the human operator applies a constant force on the local manipulator while the remote environment is modeled as a spring–damper system. The state convergence method ensures that the remote manipulator will track the manipulator trajectory even when there is a variable time delay between them.

In the case where the human operator stops applying a constant force or the remote manipulator does not interact with the environment, the position coordination error goes to zero; therefore, the position signals of both robots are also coordinated.

Another important result attained in this article is that the control strategy is independent of uncertainties in the parameters of the robot models, the human operator, and the remote environment.

In this paper a Lyapunov–Krasovskii functional was proposed in order to analyze delay-dependent stability and derive the stability criteria for the proposed control scheme. When the sign of $\dot{V}$ is undefined, the stability conclusions can be drawn after integration applying Barbalat's lemma.

In the teleoperation system shown in Fig. 2, the proposed controllers, (6), implement the system's dynamics as a function of their own states (local/remote) and of the delayed information of the state on the other side (remote/local). The delay should be interpreted, then, as perceived by the receiver, $\tau(t) = \tau_r(t)$.

In this way the bound on delay derivatives rejects past samples (the protocol discards a sample if the receiver has a more recent value) and verifies $\dot{\tau}(t) < 1$ [28].

It should be noted that for the selection of the controller's gain, it is assumed that $T_l(t)$ and $T_r(t)$ are continuously differentiable functions, which have a known upper bound T_i^+ and also a known variation $\left|\dot{T}_i(t)\right|$.

Many authors [29–32] have shown how to measure these upper bounds on the time-varying delay magnitude T_i^+ and its variation $\left|\dot{T}_i(t)\right|$ over real Internet conditions.

Finally, experimental results were presented to show the effectiveness of the control strategy.

Acknowledgments The authors are grateful for the use of the facilities of the Robotics and Automatic Laboratory at the Universidad Politécnica de Madrid and the Laboratorio de Investigación en Biomecánica y Robótica Aplicada at the Pontificia Universidad Católica del Perú. The authors would also like to thank the Spanish government's CICYT Project Ref. DPI2009-08778 and Comunidad de Madrid's BOCITY2030-II Ref. P2009/DPI-1559 for their financial support.

References

1. Goertz RC, Thompson RC (1954) Electronically controlled manipulator. Nucleonics 12:46–47
2. Hannaford B (1989) Stability and performance tradeoffs in bi-lateral telemanipulation. In: Proceedings of IEEE international conference on robotics and automation, Scottsdale, pp 1764–1767
3. Sheridan TB (1995) Teleoperation, telerobotics and telepresence: a progress report. Control Eng Pract 3(2):205–214
4. Hokayem PF, Spong MW (2006) Bilateral teleoperation: an historical survey. Automatica 42(12):2035–2057
5. Azorin JM, Reinoso O, Aracil R, Ferre M (2004) Control of teleoperators with communication time delay through state convergence. J Robot Syst 21(4):167–182

6. Ganjefar S, Momeni H, Janabi-Sharifi F (2002) Teleoperation systems design using augmented wave-variables and Smith predictor method for reducing time-delay effects, In: Proceedings of the IEEE international symposium on intelligent control, Oct 2002, pp 333–338
7. Li Z, Su C-Y (2013) Neural-adaptive control of single-master multiple slaves teleoperation for coordinated multiple mobile manipulators with time-varying communication delays and input uncertainty. IEEE Trans Neural Netw Learn Syst 24(9):1400–1413
8. Li Z, Ding L, Gao H, Duan G, Su C-Y (2013) Trilateral tele-operation of adaptive fuzzy force/motion control for nonlinear teleoperators with communication random delays. IEEE Trans Fuzzy Syst 21(4):610–624
9. Li Z, Cao X, Tang Y, Li R, Ye W (2013) Bilateral teleoperation of holonomic constrained robotic system with time-varying delays. IEEE Trans Instrum Meas 62(4):752–765
10. Li Z, Xia Y, Cao X (2013) Adaptive control of bilateral teleoperation with unsymmetrical time-varying delays. Int J Innov Comput Inf Control 9(2):753–767
11. Hashemzadeh F, Hassanzadeh I, Tavakoli M, Alizadeh G (2012) Adaptive control for state synchronization of nonlinear haptic telerobotic systems with asymmetric varying time delays. J Intell Robot Syst 68(3–4):245–259
12. Nuño E, Basañez L, Ortega R, Spong MW (2009) Position tracking for non-linear teleoperators with variable time delay. Int J Robot Res 28(7):895–910
13. Peña C (2009) Trabajo Tesis Doctoral, Control Bilateral por Convergencia de Estados para Sistemas Teleoperados con Robots de Cinemática Diferente. Universidad Politécnica de Madrid, Madrid
14. Artigas M, Aracil R, Ferre M, Garcia C (2010) Adaptive bilateral control systems through state convergence in teleoperation. RIAI - Revista Iberoamericana de Automatica e Informatica Industrial 7(3):42–50
15. Azorin JM, Reinoso O, Aracil R, Ferre M (2004) Generalized control method by state convergence for teleoperation systems with time delay. Automatica 40:1575–1582
16. Tafur JC, Garcia C, Aracil R, Saltaren R (2013) Stability analysis of teleoperation system by state convergence with variable time delay. American Control Conference, Washington, 17–19 June 2013, pp 5696–5701
17. Tafur JC, Peña C, Aracil R, Garcia C (2012) Control of a teleoperation system by state convergence with variable time delay Mecatronics-REM 2012, Paris, 21–23 Nov 978-1-4673-4772-3/12 IEEE, pp 40–47
18. Gu K, Niculescu S (2003) Survey on recents results in the stability and control of time-delayed systems. Trans ASME 125:158–165
19. Xu S, Lam J (2005) Improved delay-dependent stability criteria for time-delay systems. IEEE Trans Autom Control 50(3):384–387
20. Papachristodoulou A, Peet M, Lall S (2005) Constructing Lyapunov–Krasovskii functionals for linear time delay systems. American Control Conference, Portland, 8–10 June 2005, pp 2845–2850
21. Kelly R, Santibáñez V (2003) Control de Movimiento de robots manipuladores. Prentice Hall, Upper Saddle River
22. Spong Mark W, Hutchinson Seth, Vidyasagar M (2006) Robot modeling and control. Wiley, New York
23. Kelly R, Santibáñez V, Loría A (2005) Control of robot manipulators in joint spaces. Springer, London
24. Slotine JJ, Li W (1991) Applied nonlinear control. Prentice Hall, Upper Saddle River
25. Teel AR (1991) Asymptotic convergence from Lp stability. IEEE Trans Autom Control 44(11):2169–2170
26. Khalil HK (2002) Nonlinear systems, 3rd edn. Prentice Hall, Upper Saddle River, ISBN 0-13-067389-7
27. Tafur JC, Peña C, Aracil R, Garcia C (2010) An implemented of a real-time experimental setup for robotic teleoperation system. In: Proceedings of the 11th international workshop on research and education in mechatronics - REM 2010, Ostrava, pp 41–48, Sept 2010
28. Delgado E, Díaz-Cacho M, Bustelo D, Barreiro A (2011) Stability of teleoperation systems under time-varying delays by using Lyapunov-Krasovskii techniques. In: Proceedings of the 18th IFAC World Congress, Milano, Italy, 28 Aug–2 Sept 2011
29. Oboe R, Fiorini P (1998) A design and control environment for internet-based telerobotics. Int J Robot Res 17(4):433–449
30. Delgado E, Barreiro A (2007) Stability of teleoperation systems for time-varying delays by LMI techniques. In: Proceedings of the European Control Conference ECC 2007, Kos, Euca 978–960-89028-5-5, pp 4214–4221
31. Yokokohji Y, Tsujioka T, Yoshikawa T (2002) Bilateral control with time-varying delay including communication blackout. In: Proceedings of the 10th symposium on haptic interfaces for virtual environment and teleoperator systems (HAPTICS.02)
32. Slama T, Trevisani A, Aubry D, Oboe R, Kratz F (2008) Experimental analysis of an internet-based bilateral teleoperation system with motion and force scaling using a model predictive controller. IEEE Trans Ind Electron 55(9):3290–3299